ICE RINK PROTECTION SYSTEMS –
Improve and Apply a Numerical Model to Gain Insight in the Safety of Ice Rink Protection Systems

Document: Thesis Report
Author: Yolanda Bruinsma
Date: April 4, 2017

Ice Rink Protection Systems –
Improve and Apply a Numerical Model to Gain Insight in the Safety of Ice Rink Protection Systems

Master Thesis Mechanical Engineering
Biomechanical Design – Sports Engineering

By: Yolanda Bruinsma *(4086694)*
Y.Bruinsma@student.tudelft.nl

Project supervisors:

TU Delft
Prof. dr. H.E.J. Veeger
H.E.J.Veeger@tudelft.nl

Sidijk
Ronald Rotteveel
Ronald.Rotteveel@sidijk.nl

Abstract

Many falls occur in speed skating, most of which end up in protective padding that is placed along the ice rink. In this research project a testing method was established that can be used to test the influence of different padding parameters on the performance of the padding in relation to the skaters' injury risks. An existing numerical model was updated and validated by comparing three simulations of the model to real impact scenarios. Because the validation tests resembled the real impact scenarios quite well, the model is deemed suitable for performing more padding tests.

Furthermore, tests were done with variable air pressure and cover friction. Injury criteria for the head, neck and spine were measured. The HIC, Nkm and CTI did not show a clear correlation between one of the variables and any of the injury criteria. They did give an impression of the possible severity of the incurred injury in that impact scenario. A threshold value of 700 for the HIC, corresponding to a 30% risk of incurring an AIS ≥ 2 head injury, was exceeded by 70% of the measured values. Also quite an amount of Nkm and CTI values were above their threshold value of 1.0, which corresponds to a 25% risk of incurring an AIS ≥ 3 injury. These high injury criterion values may point towards the high risk of skaters of incurring severe injuries. However, the large amount of high values is not in proportion to the amount of severe injuries that is incurred in reality. This may be explained by the fact that a real skater can react earlier and more active to the impact than the model can.

Contents

Abstract 3
Contents 5
1. Introduction 6
1.1 Research motivation 6
1.2 Literature review 7
1.3 Report structure 7
2. MADYMO model 8
2.1 Selection of a testing method 8
2.2 Description of the MADYMO model 8
2.3 Injury criteria 12
3. Comparison of the model to real impact scenarios 15
3.1 Simulated impact scenarios 15
3.2 Conclusion on the validity of the model 19
4. Testing of padding variables 20
4.1 Simulated impact scenario 20
4.2 Testing variables 20
4.3 Results 21
4.4 Conclusion on padding variables 25
5. Discussion and conclusions 26
5.1 Discussion 26
5.2 Conclusions 27
6. Recommendations 28
References 29

Appendix A. Selection of testing method 30
Appendix B. Images of real crashes and simulations 32
Appendix C. Data from injury criteria 35
Appendix D. Images of simulated impact scenarios 38

1. Introduction

All over the world speed skating is practiced from amateur to professional level. Speed skating can be divided into two disciplines: long track and short track speed skating. Long track speed skating is performed on a 400m ice rink. There is a division into competitions with two skaters on the rink aiming for the fastest time over 500 to 10000 meters and marathon and mass start competitions with a peloton of skaters in the rink aiming for the best ranking at the finish. In short track speed skating 4 to 8 skaters race against each other over distances of 500 to 3000 meters on a 111.12m ice rink, aiming for the best ranking at the finish.

The risk of falling is high in speed skating, because of the slipperiness of the ice and the high velocities that the skaters reach (up to 60km/h). Furthermore, in short track speed skating and marathon and mass start competitions a peloton of skaters skate close to each other with the risk of touching each other causing a crash, often with more than one skater together. When skaters fall, most often they slide towards the side of the rink and hit the protective padding. These paddings have the goal to absorb the kinetic energy of the skater upon impact and minimize the risk of incurring severe injuries. In order to make sure that these paddings are in the right places and attached in the right way to ensure the safety of the skaters sufficiently, the national and international skating unions have set standards for ice rink protection systems.

1.1 Research motivation

In speed skating, severe injuries that are incurred by a crash with the padding still occur. This implies that the current protection systems are not yet safe enough. In this project the current safety measurements are reviewed and research is done to determine which method can be used to evaluate an ice rink protection system and what influence several padding parameters have on the skaters' risk of incurring injuries.

This research was initiated by Sidijk, a company in the Netherlands that designs and manufactures ice rink protection systems for both long track and short track speed skating. Paddings designed by Sidijk are intended to provide the best possible safety for the skaters. These paddings are safer than the safety measurements of national and international skating unions prescribe, because it is believed that those safety measurement do not provide sufficient safety for the skaters. Therefore, an improved set of safety measurements for ice rink protection systems is needed.

The initial project goal consists of two parts. First, there is aim for an improved standard that lists the criteria that a safe padding should meet. This requires the determination of the parameters that influence the safety of the padding and a quantification of limit values for those parameters. Secondly, a testing procedure for protective paddings is desired that can be used to objectively assess the paddings against the standards. Since both wishes require substantially different working procedures, it is decided that this project will be focused on the first part, which leads to the following research goal:

'Establish and apply a testing method to measure relevant padding parameters in relation to the skaters' injury risks.'

This project consists of two phases. In the first phase a literature review was done in order to gain insight in the injuries occurring in speed skating and the factors contributing to the severity of those injuries in relation to the impact with the safety padding. The next paragraph gives a summary of this literature review. The full review is published separately (Bruinsma, 2016).
In the second phase, a testing method is established and parameters are determined that indicate the performance of a safety padding. Testing is done to determine the influence of a variable on the injury risk of the skater. Results from this research may form the basis of an improvement of the current standards for ice rink protection systems. This report marks the end of this phase and thereby the end of the research project.

1.2 Literature review

In the first phase of this research a literature review was done in order to determine which factors are of importance for the safety of an ice rink protection system and how those factors could be measured (Bruinsma, 2016). The literature review has unveiled several important factors that can be directly used in the testing phase. Since most falls occur in the curves, a padding compartment from the curve section is used for testing. Skaters reach top speeds of 50-60km/h in the curves and when falling they hit the padding mostly under an angle of around 45°. Those values are used as a testing input. Furthermore, the padding cover should be water-resistant in order to protect the inside material and skaters should be prevented from sliding underneath the padding by keeping the attachment height of the padding to the ground as low as possible.

Several other factors have been found to be of importance for the safety of ice rink protection systems. However, for these parameters limit values still need to be determined. These parameters may be used as variables for testing in this research phase:

- Skater posture
- Movability of the padding
- Ground surface beneath a movable padding
- Air pressure in an air filled padding
- Composition of a foam filled padding
- Foam density of a foam filled padding
- Coefficient of friction of the padding cover
- Air venting in the padding cover
- Thickness of the padding cover
- Cut-resistance of the padding cover
- Stiffness of the padding cover material
- Padding dimensions (height and width)

There are several different measurement methods that were previously used for testing of ice rink protection systems. These methods have been found in the literature review:

- Drop test
- Pendulum test
- Numerical simulation
- Crash test dummy

Finally, some measurable parameters have been found in literature that can be used to judge the performance of the padding:

- Deformation
- Bounce back
- Rebound energy
- Peak acceleration
- Peak deceleration
- Energy absorption
- Injury (by an injury criterion)

1.3 Report structure

In order to reach the research goal, a measurement method needs to be chosen and experiments have to be done. Chapter 2 explains why it has been chosen to use numerical simulations for this project. Furthermore, an overview is given of the software and of the models that were used.

Chapter 3 shows a validation of the model, by comparing three real crashes to the simulations of those crashes. This gives an idea of how realistic the model can predict a skater's crash and of eventual limitations that the model has compared to reality.

Chapter 4 gives a summary of the tests that were done where padding parameters were varied in the model. It explains which parameters have been chosen for testing and concludes with conclusions on the influence of those parameters on the injury of the skater upon impacting the padding.

The report concludes with a discussion and conclusions in Chapter 5 and recommendations for further research in order to improve the standards for ice rink protection systems in Chapter 6.

2. MADYMO model

In the first phase of this research project, a literature study has unveiled several testing methods that may be used for doing the testing in this phase of the project. In this chapter the choice for a testing method is explained. Furthermore, an description is given of the numerical MADYMO modelling software and the padding model that was obtained from the previous TNO research (Forbes et al., 2006, 2007).

2.1 Selection of a testing method

In the literature review four methods were found that were used for previous testing and research on ice rink protection systems and similar protective devices:

- Drop test (ISU, 2012)
- Pendulum test (Forbes et al., 2007, Maw and Johnston, 2005, 2010)
- Numerical model (Forbes et al., 2006, 2007)
- Crash test (FIM, 2015)

Appendix A gives a description of each method and weighs the pros and cons regarding to the performance of the method in order to make a selection. The two criteria that are valued in the performance of a testing method are the representation of the padding and the representation of the skater in three aspects: the sliding motion, the body posture and the injury response. The method that scores best overall is the numerical model, because the representation of the skater by a numerical human body model is of a high level and also the padding can be modelled to an acceptable level. Therefore, for this research it has been decided to use the numerical MADYMO model to simulate the crash between a skater and the padding.

2.2 Description of the MADYMO model

The numerical modelling software that will be used for simulations in this research project is the MADYMO modelling software. This software is launched by Tass International, a company that offers virtual models, simulation software, engineering services and testing facilities that can be used for the development of safety systems for the transport industry (Tass-International, 2017).

This software, which is normally used for simulations for the transport industry, is very suitable for simulating the impact between a skater and the padding, because it includes very detailed human body models that are able to calculate injury parameters of all body parts. Furthermore, it has very extensive airbag modelling features, which are of use when building an air filled padding.

Forbes et al. (2006) built a numerical model in order to obtain recommendations for improvement of padding systems with the intention of improving the safety of long track speed skaters. The research of TNO was initiated by the Royal Dutch Skating Union (KNSB) and was in collaboration with the Dutch institute for sports accommodations (in Dutch: 'Instituut voor Sportaccommodaties (ISA)').

The model developed by Forbes et al. (2006) was built in release version 6.3. The latest release version that is used in this research project is 7.6. In order to make the model work in the latest software version, several general adjustments were made. Furthermore, a new human body model was chosen and several changes and additions were made to the padding model.

2.2.1 Human model

Forbes et al. (2006) did an extensive research of the different human body models that were available in the MADYMO software. Their selection criteria were that the model should be able to replicate the required response and injury and that the model was computational efficient. Based on those two criteria the facet human body model was chosen. That model performed good on the head, spine and shoulder region. However, it performed weak on the leg region. Therefore, the facet human body model was combined with the detailed facet leg model.

In the latest software release, new human body models are available compared to when Forbes et al. (2006) did their research. For this project the sitting version of the facet active human model was used in the size of the mid-size male (representing the 50th percentile male model population). This model is based on the former facet male model, the detailed leg model and several other detailed body part models. Therefore, it includes all features that were available in the combined model of Forbes et al. (2006) and has improved in all aspects. A major difference of this model compared to the former facet human body model is that it includes active behaviour. The neck, spine, hips and elbows have been given the property that they try to maintain their initial position (in all of their rotational degrees of freedom) under the influence of external loading (MADYMO, 2015a).

Two delays are present in the active body parts of the model. The first is the reaction time and the second is the neural delay. The reaction time is not present when it comes to controlling stabilizing errors, and is set to 100ms for responses to new events. New events occur when an external load causes a control error that is larger than the maximum error that was detected in the simulation up to the current time step. The neural delay is always present and varies by body part. The neural delay of the neck muscles is set to 40ms, for the spine and the arm muscles to 70ms and for the leg muscles to 100ms (MADYMO, 2015a).

For validation of the human model two types of data were used: volunteer test data for low to mid severity impact and post mortem human substitute (PMHS) test data for mid to high severity impact. Data of impact tests were used to validate separate body segments and data of sled tests and vibration tests were used for validation of the full body response (MADYMO, 2015a).

2.2.2 Air filled padding model

Since a model of an air filled padding was already available from research by Forbes et al. (2006), (2007) this research focuses on the air filled padding for long track speed skating. The padding section was modelled according to CAD data obtained from Sidijk. The model was constructed by a mesh of triad elements to obtain the smoothest mesh properties. The existing model was adjusted to the latest software version of MADYMO and underwent several changes of padding properties.

Dimensions

Forbes et al. (2006) used a design of a Sidijk padding to build the model. Dimensions of this padding design are still relevant. Since most accidents involving the padding happen in the curves, a curve section of the padding is used. The curve (with a radius of approximately 34 meters) is in the length divided into six padding components, each with a length of 18 meters. The padding has a height of 1.07m (when inflated) and a width of 0.6m. Padding dimensions can also be found in Figure 1.

A padding section is divided into eight rectangular air chambers, each connected with each other by holes in the interior walls. On the bottom of the padding an attachment flap is placed to attach the padding to the floor.

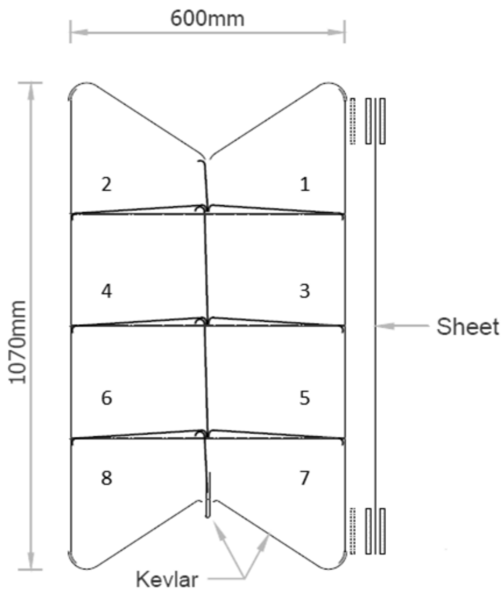

Figure 1 – Dimensions of the padding

Materials

In the old padding model, it was assumed that the whole padding was made of the same material, being POLYMAR. The material properties of a similar material, Bisonyl, were used. However, the padding is made of different materials and on the front of the padding (the side facing the ice) a sheet is attached to the padding by two Velcro straps.

The major part of the padding is made of Panama fabric, a PVC coated Polyester fabric. The bottom of the padding, including the attachment flap, is made of Kevlar material, also a PVC coated Aramide fabric, but with a higher strength. The sheet that is attached to the front of the padding is composed of two layers of Icetex fabric with one cut-resistant layer of Dyneema fabric in between.

Since the Kevlar fabric is only used for the bottom of the padding, a part that is not involved in the impact, it is assumed that those parts are made of Panama fabric as well. The Dyneema fabric in the sheet is very thin and flexible and only added to provide cut-resistance, a property that cannot be implemented in the model. Therefore, this fabric is neglected and the sheet is assumed to be composed of two layers of Icetex only.

Making these assumptions, only two fabrics are used in the model: Panama and Icetex. The failure strain for common PVC coated polyester fabrics is approximately 15% (Forbes et al., 2006). This strain is used to calculate the elastic modulus. Properties of both fabrics can be found in Table 1.

Table 1 – Material properties

	Panama	**Icetex**
Weight [kg/m²][1]	0.900	0.730
Thickness [mm]	0.70	0.75
Tensile strength [kN/m][1]	86	110
Tear strength [kN/m][1]	10	20
E modulus [GPa]	0.819	0.978

[1] Numbers by Mehler (2008), (2013)

In the model two materials are defined that are used to give the whole padding it's material properties. The fabrics are modelled as linear elastic materials. The first material is the Panama fabric that is applied to all inner and back parts of the padding. This material has a thickness of 0.70mm. Since nothing was known about the stress-strain curve of the material, the tensile strength was used to calculate the elastic modulus. For this layer a tensile strength of 86kN/m, a thickness of 0.70mm and a failure strain of 0.15 give an elastic modulus of 0.819MPa. The density of this material is 1285.7km/m^3, from a thickness of 0.70mm and a weight of 0.900 kg/m^2.

The second material is a combination of one layer of Panama and two layers of Icetex fabric. This represents the padding wall and the sheet and is used for all front parts of the padding. Since the sheet was not modelled initially, it is hard to add it to the model afterwards. Therefore, the material properties of the sheet are included in the padding wall to include the stiffness properties of the sheet. The extra pre-stress in the sheet that is caused by spanning the sheet between the Velcro straps, is not included in the model this way. This pre-stress would be hard to determine anyway, because it depends on how tight the sheet is spanned, which varies every time it is detached and attached again. The total material has a thickness of 2.2mm. Together with an elastic modulus of 0.819MPa for a 0.70mm layer of Panama and of 0.978MPa for one 0.75mm layer of Icetex, the combined elastic modulus is 0.909MPa. The density of this combined material is 1072.7kg/m^3, from a weight of 0.730kg/m^2 for one 0.75mm Icetex layer and a weight of 0.900kg/m^2 for a 0.70mm Panama layer.

Friction

Forbes et al. (2007) performed tribological experiments to measure the coefficient of friction between a skating suit and the padding materials. Both, an Icetex sheet and an advertising cover were tested. The test with the Icetex sheet showed a constant coefficient of friction of approximately 0.7. For the advertising cover the test showed varying results. The printed part of the cover gave a very low friction coefficient of 0.3, while the non-printed part gave a very high coefficient of friction of 0.9.

Air pressure

The air pressure within the padding is generated by an air fan that is connected to one single air chamber of the padding. In the model, the inflation of the padding is done using a mass flow rate function that defines the amount of air that is blown into padding in kg/s. The air is blown into the padding in air chamber 8 (see Figure 1) at the side of the padding compartment.

Forbes et al. (2007) determined a function that describes the correlation between this mass flow rate and the air pressure in the padding. This was done by performing a series of simulations with varying mass flow rates and measuring the air pressure in the padding. However, due to changes in the padding model that were made in this research project, that correlation function did not seem to match anymore. Therefore, the process of determining a correlation between the mass flow rate and the air pressure in the padding was re-done. Results of these simulations can be found in Figure 2. The air pressure in this figure, is the air pressure in the padding with respect to the environment. Ambient pressure is modelled to be 101,325Pa, which is the average ambient pressure at sea level.

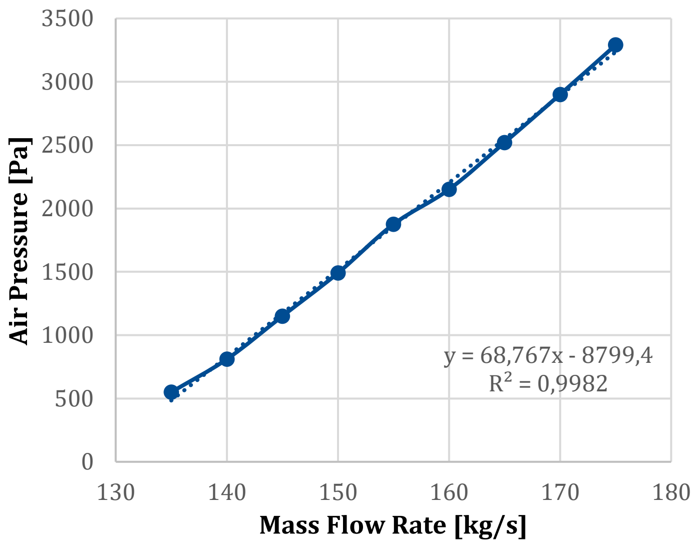

Figure 2 – Relation between the air pressure in the padding and the mass flow rate

It can be seen that the relation between the air pressure in the padding (Pa) and the mass flow rate (kg/s) is a linear relation. This relation can be described with the following function:

$$Air\ Pressure = 68.767 * Mass\ Flow\ Rate - 8799.4$$

Figure 3 shows air pressure in the eight airbag chambers of the padding over time for a mass flow rate of 150kg/s. It can be seen that at the start the air pressure is highest in airbag chamber 8 where the air is inflated. Thereafter, the air is divided over the other airbag chambers and stabilizes to a constant pressure, which is equal in all air chambers. The time at which the pressure reaches a constant level ranges from 190 to 220ms for the different mass flow rates.

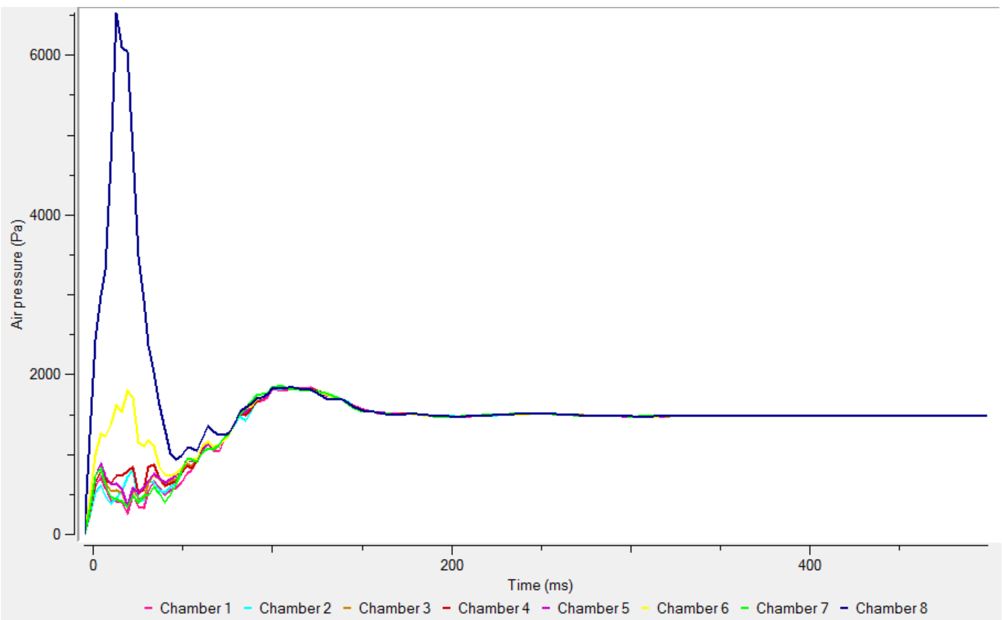

Figure 3 – Air pressure in the eight airbag chambers over time (for MFR = 150kg/s)

In a real padding, air leakage out of the padding occurs, while air fans continuously blow air into the padding to compensate and keep the pressure constant. Forbes et al. (2007) created this effect in the model by giving the padding material of the outer parts permeability properties to produce the appropriate leakage and defining an extra air inflow to keep the pressure constant. However, in this research project the leakage was taken out of the model, because without leakage and extra air inflow the pressure in the padding is already constant, and both the leakage and extra inflow would have to be changed for different mass flow rate input values.

Padding attachment to the ground

An air filled padding is always fixed to the ground. In order to do so an attachment flap is placed on the bottom of the padding. A steel rod is threaded through the flap and attached to the ground using eye-bolts. The distance between the lower side of the attachment flap and the ground is 26mm.

There are two types of padding attachment to the ground. In the first type the eye-bolts are directly connected to the floor and the padding is not able to move in any direction. In this attachment type there is a connection to the ground every 0.5m.

In the second type the eye-bolts are connected to slide anchors that are fixed in the floor. These slide anchors allow for movement in the horizontal plane by a system of two compression springs. Therefore, the padding is able to move outwards upon impact in order to provide better impact absorption. In this attachment type there is a slide anchor placed every 0.73m.

Simulations in this report were all done using the fixed connection method, since the slide anchors were not yet implemented in the model.

2.3 Injury criteria

In the literature review several injury criteria were observed that can describe the relation between the impact of the skater with the padding and the injury risk. For this research project the focus is on injuries to the head, neck and spine region. All injury criteria that were observed are correlated to the Abbreviated Injury Scale (AIS). This scale describes the severity of an injury on a scale of one to six, with one being a minor injury like a headache or abrasions and six being an injury that is so severe that it leads to death (Shojaati, 2003). All levels of the AIS are described in Table 2.

Table 2 – The AIS scale with examples of head and spinal injuries[1]

AIS	Level	Injury examples
1	Minor	Headache (no unconsciousness), whiplash, abrasions, contusion
2	Moderate	Concussion (<15 min. unconscious), tiny corneal cracks, retinal detachment, non-shifted face or nose fracture
3	Serious	Concussion (>15 min. unconscious), loss of vision, open and/or shifted face bone fracture, cervical fracture without spinal cord damage
4	Severe	Skull fracture with severe neurological injuries
5	Critical	Concussion (>12 hrs. unconscious) with critical neurological indications and/or haemorrhage in skull
6	Survival not sure	Death, partly or full damage of the brainstem or upper cervical, fracture of the upper cervical with spinal cord injury

[1]Data from Shojaati (2003)

This paragraph describes the injury criteria that have been selected for this research.

2.3.1 Head Injury Criterion (HIC)

The Head Injury Criterion (HIC) is based on the linear acceleration of the head over a certain time interval, and is therefore very suitable for assessment of the concussion tolerance. The HIC is calculated by the following formula (Eppinger et al., 1999):

$$HIC = max\left\{\left[\frac{1}{t_2 - t_1}\int_{t_1}^{t_2} a(t)\,dt\right]^{2.5}(t_2 - t_1)\right\}$$

In this formula, a(t) is the resultant head acceleration [g] over a time span (t_2 - t_1) [s], which should be chosen to be maximal 15 or 36ms. The shortest of these intervals is introduced to restrict the use of HIC to hard impacts (MADYMO, 2015c). The criteria calculates a maximum value and gives that value as an output together with the time span at which the maximum value occurs.

Figure 4 shows the relationship between the HIC value and the probability to obtain a moderate to serious head injury (AIS ≥ 2). This level of injuries refers to more serious concussions and fractures of the facial bones. For the HIC with a time duration of 15ms a maximum threshold value of 700 is proposed (Eppinger et al., 1999). This corresponds to a 30% risk of incurring an AIS ≥ 2 head injury, as can be seen in Figure 4.

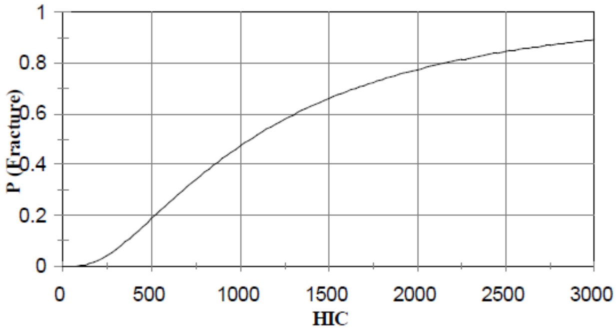

Figure 4 – Probability to obtain a moderate to severe head injury (AIS ≥ 2) (Eppinger et al., 1999)

2.3.2 Neck injury predictor Nkm

Nkm is a neck injury predictor based on a combination of shear forces in the neck and the moment about the occipital condyle. Nkm is described by the following formula (Schmitt et al., 2001):

$$N_{km}(t) = \frac{F_x(t)}{F_{int}} + \frac{M_y(t)}{M_{int}}$$

The shear force F_x [N] and flexion or extension moment M_y [Nm] are normalized by comparing them to their critical intercept values, F_{int} and M_{int} respectively for each time, t. For the mid-size male dummy size MADYMO uses a value of 845N for the positive or negative shear force F_x, a value of 88.1Nm for the flexion moment M_y and a value of 47.5Nm for the extension moment M_y (MADYMO, 2015b).

This injury criterion is a collective of four injury predictors for different combinations of the shear force and bending moment:

- N_{fa}: flexion moment (M_y>0) and anterior shear forces (F_x>0)
- N_{ea}: extension moment (M_y<0) and anterior shear forces (F_x>0)
- N_{fp}: flexion moment (M_y>0) and posterior shear forces (F_x<0)
- N_{ep}: extension moment (M_y<0) and posterior shear forces (F_x<0)

For all four combinations a value of 1.0 is taken as a maximum for this criterion (MADYMO, 2015b).

2.3.3 Combined Thoracic Index (CTI)

The Combined Thoracic Index (CTI) is a measure for injuries of the thorax. This criterion compares the maximum spine acceleration (A_{max}, [m/s²]) and the maximum chest deflection (D_{max}, [m]) to their critical intercept values, A_{int} and D_{int} respectively. CTI is calculated using the following formula (Eppinger et al., 1999):

$$CTI = \frac{A_{max}}{A_{int}} + \frac{D_{max}}{D_{int}}$$

Critical intercept values A_{int} and D_{int} are used to normalize the maximum acceleration and chest deflection. For the mid-size male dummy size MADYMO uses a value of 805m/s^2 for the chest acceleration A_{int} and a value of 0.102m for the chest deflection D_{int} (MADYMO, 2015b). Because this criterion is based on the maximum spine acceleration and the maximum chest deflection, which do not necessarily occur at the same time, the output gives only one value. The MADYMO model calculates this criterion for four rib levels and for three sides of the body, left, right and total.

Figure 5 shows the relation between the CTI and the probability to obtain a serious to severe thoracic injury (AIS ≥ 3). The lower curve should be observed. As can be seen in the figure, a threshold of 1.0 for the CTI corresponds to a 25% risk of incurring an AIS ≥ 3 thoracic injury.

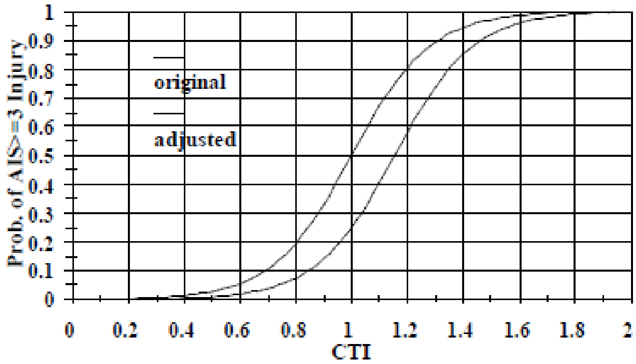

Figure 5 – Probability to obtain a severe to serious thoracic injury (AIS ≥ 3) (Eppinger et al., 1999)

3. Comparison of the model to real impact scenarios

Before a numerical model can be used to perform real tests, it should be validated. The basis of the model that is used in this research project was obtained from earlier research by Forbes et al. (2006), (2007). They validated the model by comparing results of numerical simulations to the results of experimental pendulum tests. Results for acceleration, velocity and displacement of the pendulum and pressure in the air filled padding were compared. The performance of the model was considered sufficient for the purpose of the concerned research based on those factors (Forbes et al., 2007).

In this research project, an additional validation of the adjusted model was done by comparing simulations of the model to images of real impact scenarios. In order to do so three crashes were chosen that occurred in Thialf in the skating season 2016/2017. A comparison is made based on images and animations, since no measurable data are known about the real impact scenarios. The skater posture and impact angle and speed were modelled as accurate as possible based on images of the real scenario right before impact. For the first 200ms after impact, the response of the skater is compared to images of the real impact scenario in terms of direction of the bounce back and rotation of the body. After those 200ms, the real skater shows reactive behaviour, which is not included in the model. Therefore, outcomes of the model are not comparable anymore after that time.

This chapter describes the chosen impact scenarios and concludes with a comparison of the simulations to those scenarios.

3.1 Simulated impact scenarios

All chosen impact scenarios occurred in the skating season 2016/2017 in a national or international event that was held in Thialf. The air filled padding was modelled to resemble the real padding of Thialf as good as possible. The materials of the Thialf padding are as modelled in Chapter 2.2.2 and the air pressure in the curve section of the padding was 650Pa in the relevant skating season (B. Boomsma 2017, personal communication, January 22). There is one major difference between the Thialf padding and the padding model used for these simulations. The Thialf padding is attached to the ground by slide anchors, while the model uses a fixed connection. This is because the slide anchors were not included in the model in this stage of the research.

3.1.1 Impact scenario 1

The first scenario is of a skater who fell in the outer lane of the 1500m. He slid towards the padding in a sitting position, leaning far back, with his right side hitting the padding first. Figure 6 shows how the skater was modelled based on an image of the skater at the moment of impact and an image of the simulation at 200ms after impact. The impact angle for this scenario was set to 30 degrees and the speed to 50km/h (based on an average speed on the 1500m). The skater hits an advertising cover that is half coated. Therefore, the friction coefficient was set to 0.6.

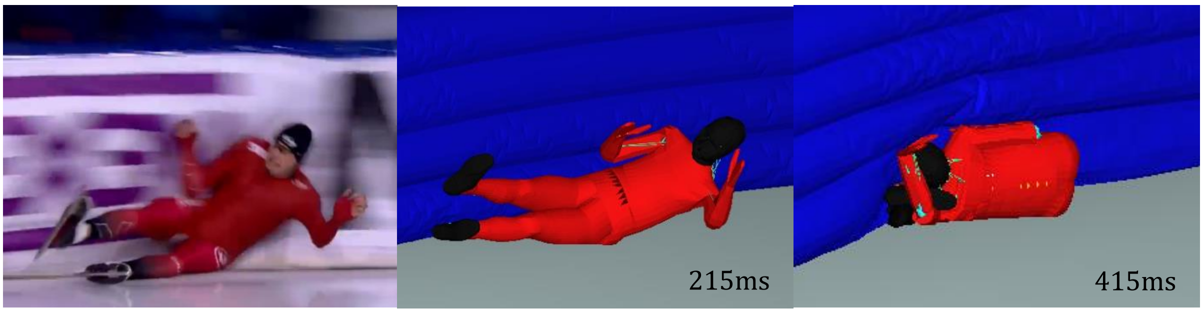

Figure 6 – Impact position of scenario 1
(left: real impact (ISU, 2016); middle: simulated impact at 215ms; right: simulated impact at 415ms)

A series of images of the impact can be found in Appendix B.1. In the real impact the skater slides towards the padding in a sitting position, hitting the padding with the right side first. Thereafter, he slides and rotates past the padding, such that he bounces back straight from the padding. At the end of his crash, the skater is in a lying position and his body has rotated almost 180 degrees.

In the images of the simulation it can be seen that the bounce back and the rotation of the skater are both present in the movement of the modelled skater right after the start of the impact. The bounce back is in the same direction as the real impact, and also the skater has rotated 180 degrees. In the images it can be seen that the skater bounces back in a position where his body is folded. Since it takes the skater circa 200ms to react to the impact, only the first 200ms after impact are relevant for comparison. This is from 215ms to 415ms. Looking at the position at 415ms, the skater just starts bouncing back. It is likely that after that time the skater makes an active effort to get his body straight again, while the model remains in a folded position.

The HIC value of this simulation is 206.48 measured between 326 and 341ms. This is far below the threshold value of 700. Figure 7 shows the Nkm development during the impact. It can be seen that the main neck movement is an extension moment with posterior shear force around 350ms. A value of 2.08 is reached, which is twice as high as the threshold value. The second peak that can be seen is of a flexion moment with anterior shear force. This occurs circa 50ms later and reaches a value of 1.00.

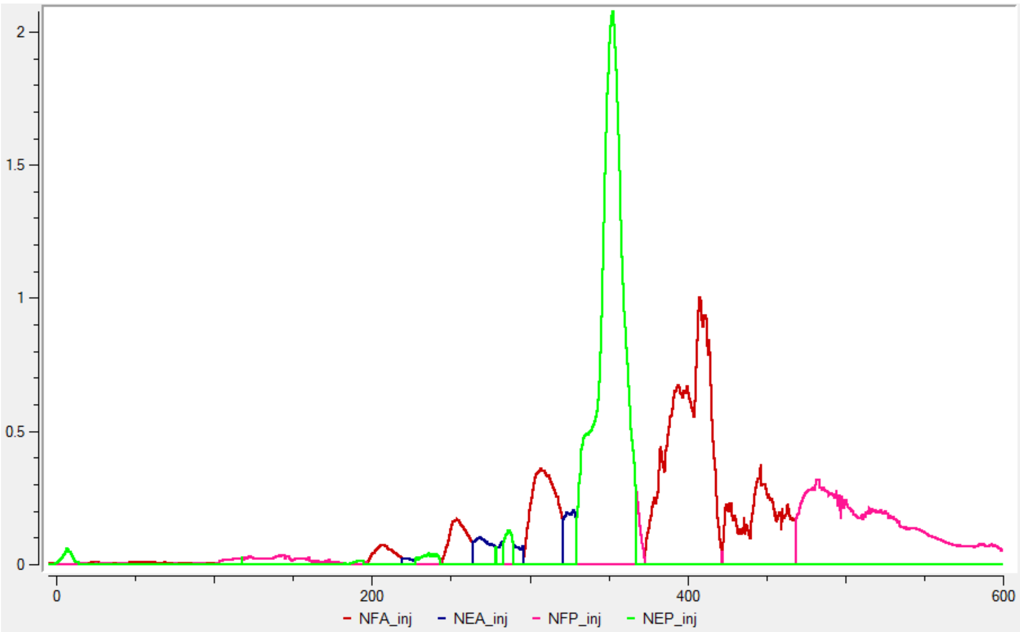

Figure 7 – Nkm for impact scenario 1

Table 3 shows all CTI values for this impact scenario. It can be seen that all values are below the threshold value of 1.0.

Table 3 – CTI values for impact scenario 1

	Rib layer 1	Rib layer 2	Rib layer 3	Rib layer 4
Total	0.71612	0.31516	0.31941	0.36203
Right	-	0.29786	0.30289	0.55449
Left	-	0.27933	0.29642	0.33975

3.1.2 Impact scenario 2

In the second scenario a skater fell in the inner lane of the 1000m. He slid towards the padding in a sitting position, leaning back with his feet up, with his right arm and shoulder hitting the padding first. Figure 8 shows images of the real impact position and the modelled position right before impact and of the simulation at 415ms. The impact angle for this scenario was set to 50 degrees and the speed to 54km/h (in accordance with the speed given by the information panels in Thialf). The skater impacts an advertising cover that is mostly coated and therefore the friction coefficient was set to 0.5.

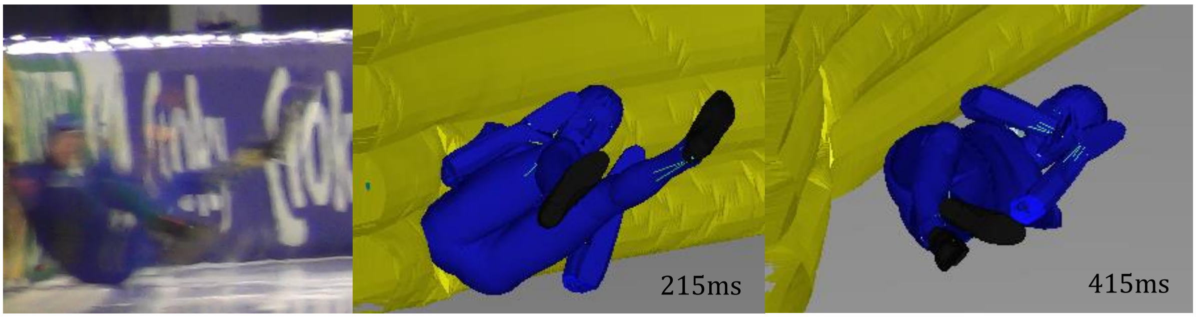

Figure 8 – Impact position of scenario 2
(left: real impact (KNSB, 2017); middle: simulated impact at 215ms; right: simulated impact at 415ms)

Appendix B.2 shows a series of images of this impact scenario. It shows a similar impact as compared to the first impact scenario. The skater slides in a sitting position, hitting the padding with the right arm and shoulder first. Thereafter, he also slides past the padding, while making a rotational motion and, like the skater in impact scenario 1, ends up with his body 180 degrees rotated.

In the images of the simulation it can be seen that the modelled skater does bounce back from the padding, like the skater in the real impact did. However, in the simulation of this impact scenario no rotation of the skater's body is seen. This may be due to the initial position of the modelled skater, which might be so that the body does not hit the padding like in the real impact. Another reason to explain this, may be that the skater in the real impact had an initial rotational velocity at the moment of impact, due to his movement in the sliding phase. In the simulation, the skater was only given an initial linear velocity in a straight line towards the padding.

A HIC value of 662.88 is calculated for this impact scenario, between 268 and 279ms. This is below the threshold of 700. A time history graph for the Nkm is shown in Figure 9. The largest peaks are seen for an extension and flexion moment, both with posterior shear force. These two peaks occur short after each other, at 270 and 280ms respectively, and both slightly exceed the threshold of 1.0 (1.16 and 1.03).

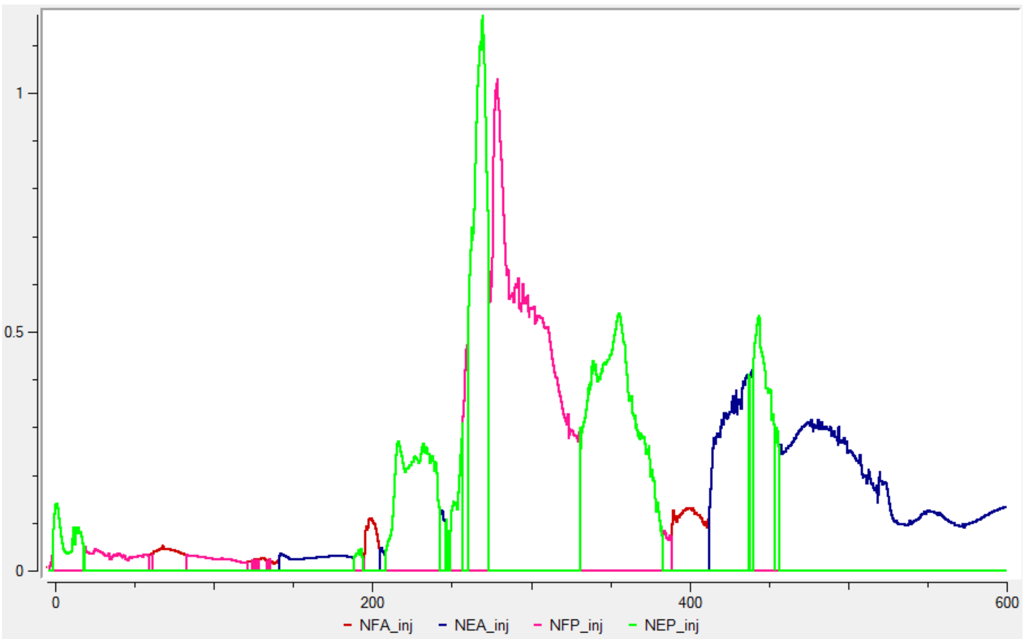

Figure 9 – Nkm for impact scenario 2

Table 4 shows CTI values for the second impact scenario. All values, except for one, are below the threshold. The CTI of the fourth rib layer slightly exceeds the threshold of 1.0.

Table 4 – CTI values for impact scenario 2[1]

	Rib layer 1	Rib layer 2	Rib layer 3	Rib layer 4
Total	0.97573	0.83145	0.72729	1.04000
Right	-	0.74938	0.74041	0.78395
Left	-	0.71138	0.74772	0.69517

[1]Values that exceed the threshold of 1 are marked in red

3.1.3 Impact scenario 3

The last impact scenario is of a skater falling in the team pursuit, a distance at which skaters skate in a group of three in the inner lane. He impacts the padding in a lying position with his legs first. Images of the skater's position and the position of the model just before impact and the simulation at 200ms after impact can be seen in Figure 10. The impact angle for this scenario was set to 45 degrees and the speed to 46km/h (the average speed for a lap time of 31.1s/400m). The skater impacts an advertising cover that seems to be mostly coated and therefore the friction coefficient was set to 0.5.

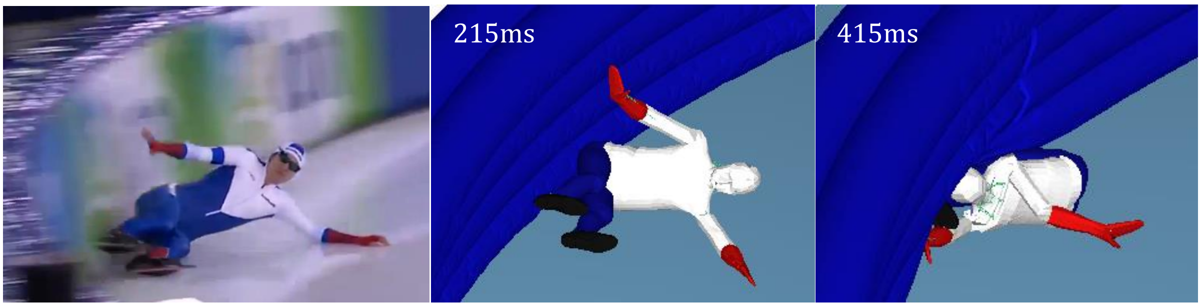

Figure 10 – Impact position of scenario 3
(left: real impact (ISU, 2016); middle: simulated impact at 215ms; right: simulated impact at 415ms)

A series of images of the third impact scenario can be found in Appendix B.3. The skater in this impact scenario slides towards the padding in an almost lying position, impacting with the feet first. He doesn't bounce far back from the padding and his body makes a small rotation, but only at the end of the impact.

The simulation of this impact scenario shows a small and straight bounce back and a very small body rotation, like was seen in the real impact. While the feet of the skater are restrained by the padding, his body moves a bit further, bending towards the feet. This effect was also seen in the real impact, however, there the body bends up towards the padding, instead of to the feet. The skater might be actively doing this, by pushing his body upwards with his left arm.

For this impact scenario a HIC value of 822.74 was calculated between 326 and 341ms. This value exceeds the threshold of 700. Figure 11 shows the Nkm for this impact scenario. A high peak of 2.75 is seen for the extension moment with posterior shear force at 322ms. Thereafter, a wider peak is seen for the flexion moment with anterior shear force that is also exceeding the threshold of 1.0, with a maximum measured value of 1.54.

In Table 5, CTI values for the third impact scenario can be seen. None of these values exceed the threshold value of 1.0.

Table 5 – CTI values for impact scenario 3

	Rib layer 1	Rib layer 2	Rib layer 3	Rib layer 4
Total	0.66462	0.41392	0.43012	0.81940
Right	-	0.55073	0.37221	0.47716
Left	-	0.44418	0.34006	0.46064

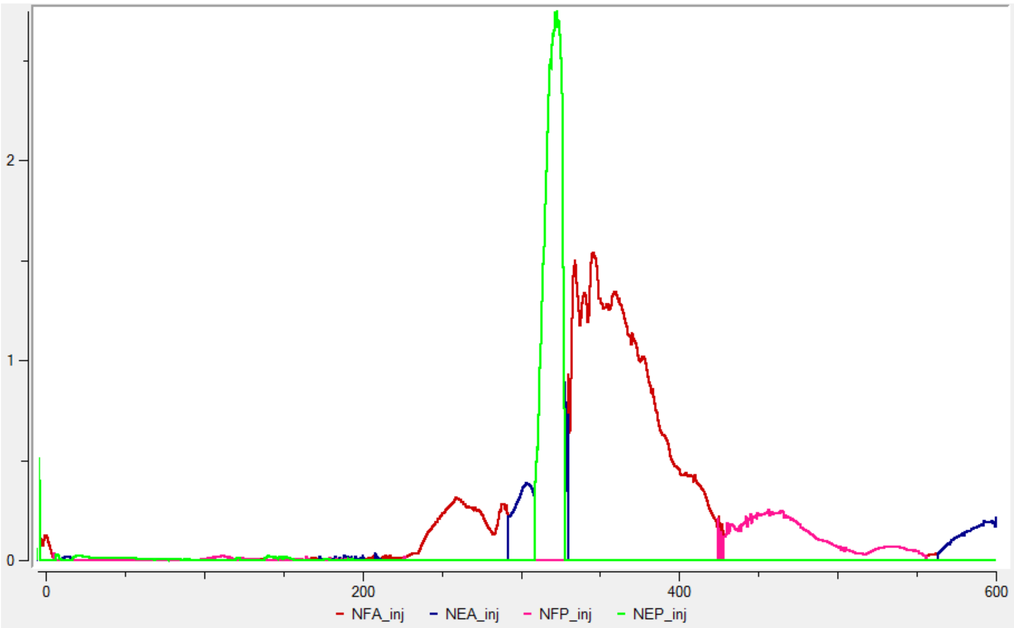

Figure 11 – Nkm for impact scenario 3

3.2 Conclusion on the validity of the model

In all three cases it was seen that the direction of bounce back in the model resembles the direction of bounce back in the real impact scenario. However, when it comes to the rotational motion of the body upon and after impact, differences are seen in the three scenarios. In impact scenario 1 a body rotation of 180 degrees was modelled quite accurate, while in impact scenario 2 the 180 degrees rotation from the real impact was not seen at all in the simulation. This shows that more factors may be of influence for the movement of the skater upon impact than were modelled in the simulations. Differences may lay in a small deviation of the modelled posture or in initial rotational velocities present in the skater's body that were not taken into account in the model. However, although the motion that was shown in the simulation of the second impact scenario doesn't resemble the real skater's behaviour, it is deemed to be a realistic response for a similar real impact scenario.

When it comes to injury criteria, it can be seen that especially the Nkm values exceed their threshold values in all impact scenarios. A possible explanation for that is that a skater may already show stiff active behaviour in the neck upon impact, because he sees his crash coming. In the model active behaviour in the neck only starts at the time of impact, from which it takes 140ms before the neck really reacts, due to the reaction time and the neural delay.

For HIC, widely varying values are seen for these three impact scenarios. This indicates that the HIC, and thus the risk of incurring a head injury, depends on the impact posture. The Nkm data show that for each simulation, two clear peaks are present. Peak values lie all in the same range, but there is a difference for which injury predictors show a peak. All simulations show a peak for an extension moment with posterior shear force. The second peak is of a flexion moment for all simulations, but twice with anterior shear forces and once with posterior shear forces.

Overall, the three impact scenarios are simulated quite well by the numerical model. Most aspects of the real impact are resembled in the simulations to a very acceptable level. Moreover, for the case where the model showed a large difference as compared to the real scenario, the modelled behaviour in that simulation was still believed to show a possible response. Therefore, the present model is deemed to perform sufficiently for the purpose of testing padding variables. When interpreting the injury criteria, one should keep in mind that the model only reacts to an external load from the moment of impact. From that moment, it takes at least 140ms until the body really reacts, where a real skater sees his crash coming and can already prepare active reaction before the start of the impact.

4. Testing of padding variables

After the validation of the model, several padding variables were tested, by varying them for one impact scenario. The performance of every combination of variables is evaluated by the injury parameters for the head, neck and spine. This chapter describes which impact scenario is used and which padding properties are varied. It concludes with an overview of the results of these tests.

4.1 Simulated impact scenario

In the literature review (Bruinsma, 2016) it was found that most skaters impact the padding in a sitting or lying position with the back or the side first. Since all three of the impact scenarios defined in the previous chapter apply to one of these most occurring postures, one of those postures was chosen for further simulations in this research project. Impact scenario 2 is used, where the skater is sliding towards the padding in a sitting position, leaning back with the feet up and hitting the padding with the right arm and shoulder first.

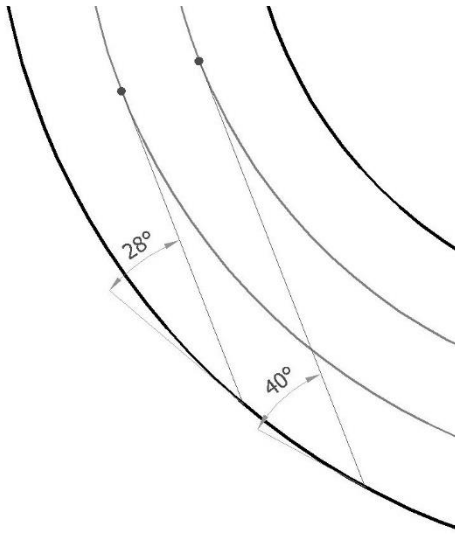

Figure 12 – Impact angles after a fall

The literature review showed that most of the falls occur in the inner lane (72%), and in Figure 12 it can be seen that when a skater would slide from the inner lane in a straight line to the padding, he would make an impact angle of 40°. This corresponds to the conclusion from the literature review that the most common impact angle is around 45°, considering that due to deceleration and friction with the ice, the skater wouldn't slide in a straight line, but with a slight curve. An angle of 45° is used for the standard impact scenario.

The literature review also showed that skaters reach top speeds of 50-60km/h in the curves. Therefore, a speed of 55km/h is used.

4.2 Testing variables

In order to test the protective properties of the padding, several padding properties were varied. The literature review has revealed a list of padding properties that may influence the safety of ice rink protection systems:

- Movability of the padding
- Ground surface beneath a movable padding
- Air pressure in an air filled padding
- Composition of a foam filled padding
- Foam density
- Coefficient of friction of the padding cover
- Air venting in the padding cover
- Thickness of the padding cover
- Cut-resistance of the padding cover
- Stiffness of the padding cover material
- Padding dimensions (height and width)

Since variation of all padding properties that are listed above would take too much time to fit into the duration of this project, two parameters were chosen to be varied in this project. This research applies to an air filled padding and it is intended to first investigate padding properties that can be easily adjusted in existing paddings. Therefore, the air pressure in the padding and the coefficient of friction of the padding cover or sheet were selected as properties to be varied.

Because the padding properties may be dependent on each other, all possible combinations of 5 values for the air pressure and 4 values for the friction are tested. This gives a total of 20 simulations.

4.2.1 Air pressure

In the research by Forbes et al. (2007), the air pressure in the Thialf padding was measured to be 1700Pa during competitions and 3000Pa during training hours. In this research the air pressure in the Thialf padding was found to be 650Pa for all events occurring at the rink. These are widely differing values. Therefore, the five values that are used for air pressure are:

- 600Pa
- 1200Pa
- 1800Pa
- 2400Pa
- 3000Pa

4.2.2 Friction

The friction between the skater and the padding depends on the materials that are being used. Forbes et al. (2007) determined that the coefficient of friction between the skater suit and Icetex fabric, which is commonly used for padding sheets, is approximately 0.7. For the advertising covers the coefficient of friction is much harder to determine, because it highly depends on the coating of the cover. Parts that are not coated at all have a coefficient of friction up to 0.9, while parts with a smooth coating have a coefficient of friction of only 0.3. It is thinkable that for different coatings, the resulting coefficient of friction may lie somewhere in between those values. Therefore, it is tested what the influence of the coefficient of friction is on the injury risk of the skater for friction values between 0.3 and 0.9. The four values that are used for the friction are:

- 0.3
- 0.5
- 0.7
- 0.9

4.3 Results

The performance of the padding is evaluated using three injury parameters for the head, neck and spine. This paragraph sums up the results for all 20 combinations of air pressure and friction expressed in values for those injury criteria.

In all simulations, the impact occurred around a time of 230ms. A skater needs approximately 200ms to react to this impact. Because this reactive behaviour is not included in the model, only the results between 230 and 430ms are taken into account. For the HIC this means that only values that lie between these times are reviewed. Because CTI doesn't give times as an output, it cannot be determined whether calculated values for this criterion have occurred during this time window. For Nkm also only peak scores within the relevant time frame are observed.

4.3.1 Head Injury Criterion (HIC)

The Head Injury Criterion is a measure for the linear acceleration of the head, and can therefore be a predictor of concussions. In Chapter 2.3.1 it was described that a threshold value of 700 for the HIC indicates a risk of 30% to incur an AIS ≥ 2 head injury, corresponding to a moderate concussion or worse. In this research project the HIC-15ms is used, because this shortest version of this criterion is introduced especially for hard impacts. The criterion gives the maximum value over a time span of 15ms. Results of the HIC are shown in Figure 13. Exact numbers can be found in Table 7 in Appendix C.1.

It becomes immediately clear that there is no correlation between the HIC and the air pressure for the modelled impact scenario. It can be seen that in general the lowest HIC values occur for a friction of 0.3, which is the only friction value for which only one value exceeds the threshold. A friction of 0.5 scores worst, with all values exceeding the threshold.

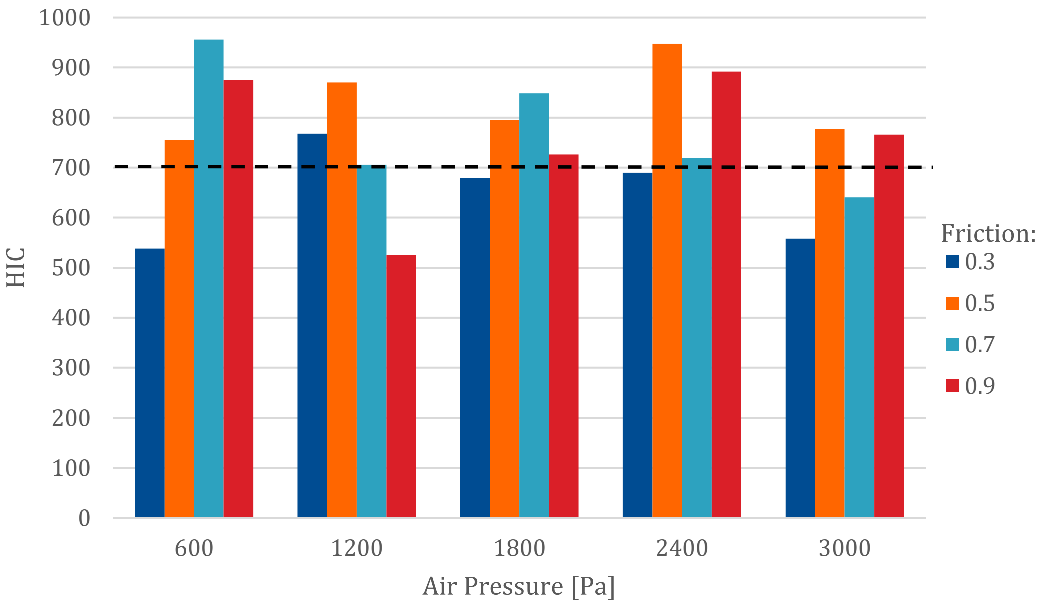

Figure 13 – HIC-15 values for all combinations of air pressure and friction

Most of the HIC values (70%) exceed the threshold of 700, with a maximum value of 955.72. In Figure 4 it can be seen that a HIC value of 1000 corresponds to a 50% risk of incurring an AIS ≥ 2 injury. Skaters impacting the padding with this impact scenario thus have a risk of 30 to 50% of incurring a moderate concussion or worse according to these HIC values.

4.3.2 Neck injury predictor Nkm

The neck injury predictor Nkm comes in four variants, each corresponding to a combination of a bending moment and a shear force in the neck. A typical time history graph of the Nkm for this impact scenario can be found in Figure 14. It can be seen that this graph shows two high peaks within the time window of 230-430ms. Therefore, peak values of this injury predictor are observed.

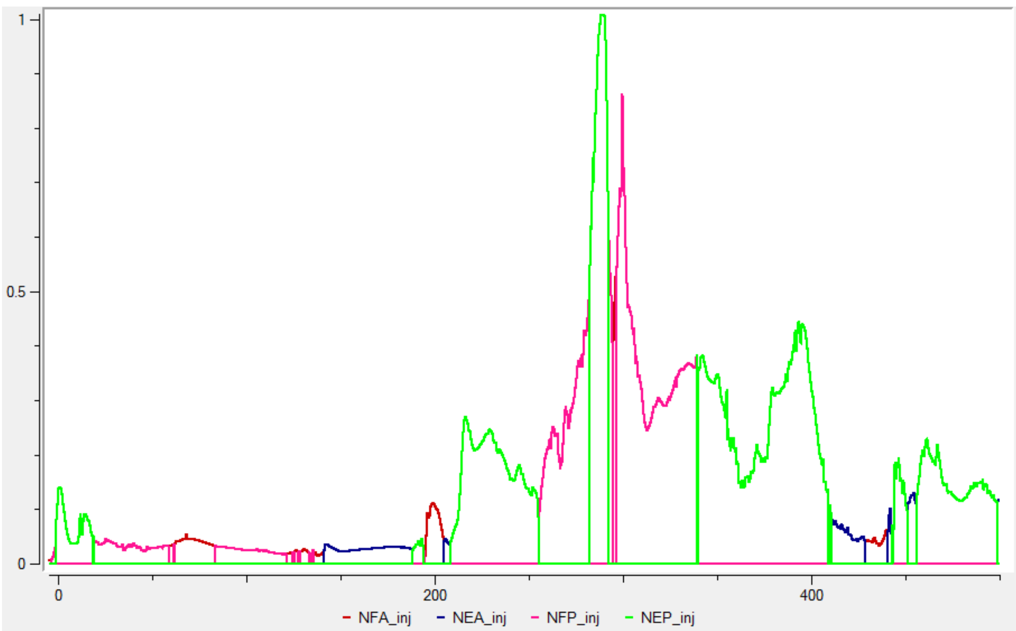

Figure 14 – Nkm for impact with friction=0.5 and air pressure=2400Pa

The NFA and NEA represent respectively a flexion and extension moment each with an anterior shear force. These injury predictors are represented by respectively the red and the blue line in the graph. Maximum values for both of these predictors can be found in Table 8 of Appendix C.2.

For the NFA only half of the maximum values occur within the time window of 230 to 430ms. All of the values that lie outside that time window are far below the threshold of 1 and the values within the relevant time window vary from 0.32 to 0.95 with one outlier of 1.11. For the NEA all but one value lie outside the relevant time window. Furthermore, all NEA values (including the one that lies in between 230 and 430ms) are far below 1, with a maximum of 0.51. These values for NFA and NEA show that the movement of the neck with anterior shear forces is negligible for this impact scenario.

Opposite to the predictors for bending moments with anterior shear forces, the predictors for bending moments with posterior shear forces show high values. The NPF and NEP are represented by respectively the pink and green line in the graph. Maximum values for these injury predictors can be found in Table 8 of Appendix C.2. NFP and NEP both show one high peak. The times at which these peaks occur give an idea of the motion of the neck after impact. The first maximum that occurs is of the NEP at an average time of circa 60ms after impact. The maximum of the NFP follows on average 9ms later. This tells us that circa 60ms after the start of the impact the neck first reaches maximum extension, shortly followed by maximum flexion, both with a posterior shear force.

Figure 15 shows the maximum values for the NFP. In general, it can be seen that the NFP increases over air pressure. For the lowest air pressure values, the NFP doesn't reach the threshold value of 1, while for the highest air pressure values the NFP exceeds the threshold several times. This pattern is seen for each individual friction value, except for the highest. For a friction of 0.9 the NFP decreases when air pressure increases. For this injury predictor, six values exceed the threshold of 1.0 of which four with a considerable amount.

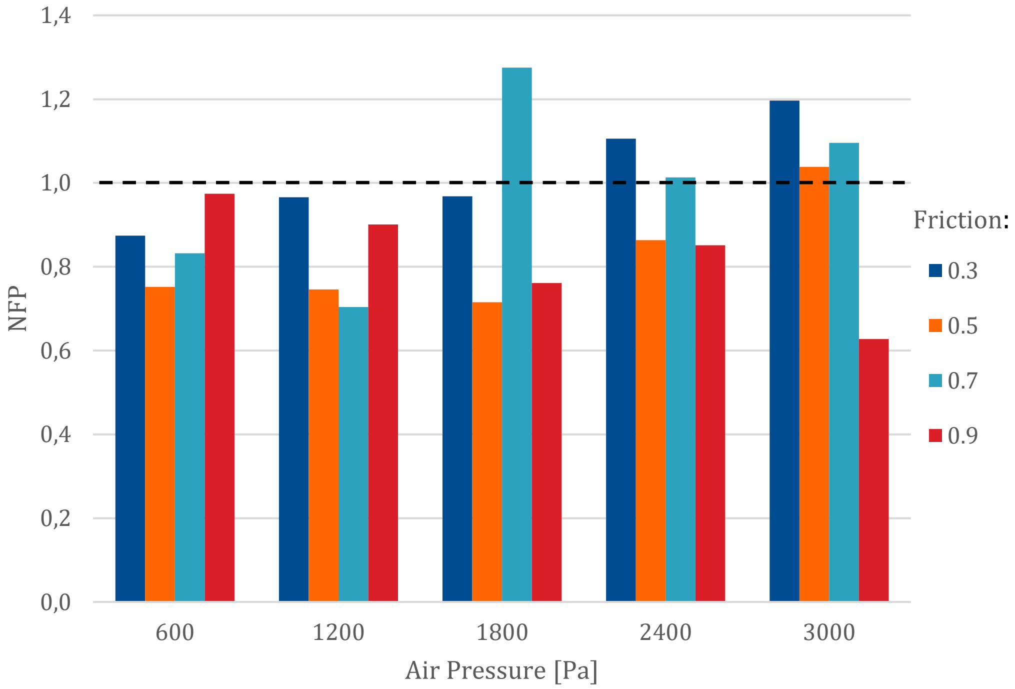

Figure 15 – Maximum NFP values for all combinations of air pressure and friction

For the NEP a different pattern is observed. Figure 16 shows that the only air pressure value without exceeding NEP values is the highest pressure of 3000Pa. The lowest air pressure values show the most exceeding values, with the three highest peaks for a friction of 0.7. In total, nine NFP values exceed the threshold of 1.0.

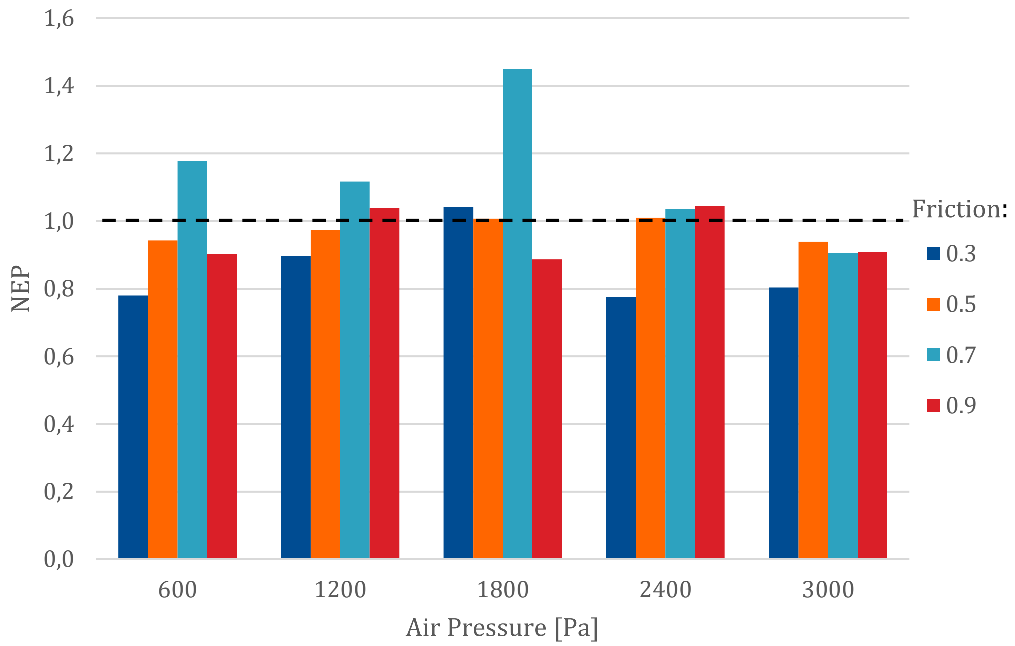

Figure 16 – Maximum NEP values for all combinations of air pressure and friction

4.3.3 Combined Thoracic Index (CTI)

The combined thoracic index (CTI) is related to the maximum spine acceleration and the maximum chest deflection. In MADYMO, this index is measured at four different rib levels and for three sides of the body: left, right and total. Table 9 to Table 12 in Appendix C.3 show all data for the CTI.

The CTI data show a very monotone pattern for all combinations of air pressure and friction and for all rib layers. Most values lie between 0.6 and 1.0 and are therefore below the threshold value of 1.0. A pattern was sought in the data for a possible correlation over air pressure, friction, rib layer or side, but for none of these factors such a correlation was found.

Circa 20% of the values in the dataset lie above the threshold value. That is an amount of 42 values. It is noticeable that 20 of these values are found within one rib layer. All combinations of air pressure and friction give a value >1 for the fourth rib layer. This may have something to do with the initial posture of the skater, who is bending his upper body far forward at the time of impact, while chest deflection is one of the parameters used for calculating this criterion. Most of the values that exceed the threshold lie between 1.0 and 1.05. According to Figure 5 these values indicate a risk of 25 to 30% to incur an AIS ≥ 3 thoracic injury. Only 7% of the CTI values predict a more severe injury, with a maximum value of 1.64 indicating a 95% risk of incurring an AIS ≥ 3 thoracic injury.

4.3.4 Penetration into the padding and body rotation

Besides an analysis of the injury criteria for all different combinations of air pressure and friction, it is also interesting to have a look at general aspects how far the skater penetrated into the padding and how his body rotates during the impact for some extreme cases. Appendix D shows images from the simulations of the four extreme combinations:

- Air pressure = 600Pa; friction = 0.3
- Air pressure = 3000Pa; friction = 0.3
- Air pressure = 600Pa; friction = 0.9
- Air pressure = 3000Pa; friction = 0.9

The images of the simulations do not show a difference in bounce back and body rotation for different friction values. On the other hand, a clear difference can be seen for different air pressure values. For both the high and the low friction it can be seen that at 235ms the skater starts impacting the padding. At 285ms both skaters have dug themselves into the padding. In the next time step, at 335ms, a difference can be noticed. In the simulation with the lowest air pressure, the skater digs himself further into the padding, while in the simulation with the highest pressure, the skater already starts coming out of the padding. In the next time steps it can be noticed that the skater impacting the low pressure padding runs almost one step behind as compared to the skater impacting the high pressure padding. Finally, the last time step, 485ms, shows that the skater impacting the high pressure padding has bounced back further that the skater impacting the low pressure padding at that time.

When observing the penetration of the skater into the padding, it should be kept in mind that in the current padding model the sheet that is attached to the front of the padding was not modelled. Stiffness properties of the sheet materials were included in the model, but the pre-stress that is caused by spanning the sheet between Velcro straps on the padding wasn't. Therefore, the front of the padding is less flexible in reality than it is in the current model. A skater will penetrate the padding less far, but this is the case for all simulations. Therefore, the difference between a low and a high air pressure that was observed in the simulations will be present in a real padding, but penetration will be less far in all cases.

4.4 Conclusion on padding variables

The three injury criteria that were observed in this testing phase do not show clear correlations between the air pressure and friction on the one hand and the injury severity on the other hand for this impact scenario. They do, however, give an idea of how severe injuries a skater may incur in a similar impact scenario.

The three injury criteria generally show high values. Most HIC values (70%) lie above the threshold of 700 and thus indicate a risk of more than 30% to incur a AIS ≥ 2 head injury. The highest HIC values point to a change of up to almost 50%. For the relevant neck injury predictors NFP and NEP 37.5% of the values exceed the threshold of 1.0, of which 17,5% by a considerable amount. Maximum values of the CTI indicate that in most cases a skater has a risk of up to 30% to incur an AIS ≥ 3 thoracic injury, though a few outliers are present pointing towards a risk of up to 95%.

Though, severe injuries happen in speed skating every now and then, the amount of injury criteria that exceeds the threshold value in these simulations is remarkably high. These high values are measured over all simulations, and show no correlation for friction or air pressure. It was already mentioned in the conclusion of the previous chapter that a real skater can start preparing an active reaction to impact before the impact occurs, because he sees his crash coming. Therefore, he can already tighten his muscles at the moment of the impact. The model only starts behaving actively when the impact starts. Then, extra tightening of the muscles comes too late, because there is a total delay (reaction time and neural delay) of at least 140ms. This may make a difference in the injury that is incurred upon impact, and may give an explanation for the large amount of high injury criteria values and the low amount of severe injuries happening in reality.

Besides the peak values of the Nkm, the time history graph of this injury predictor gives insight in the neck movement occurring upon impact. Apparently the neck first reaches maximum extension, shortly followed by maximum flexion, both with posterior shear forces. For flexion the lowest values are observed for the lower air pressure values. For extension, the higher air pressure values show the lowest NEP values. Anterior shear forces seem to be negligible in this impact scenario.

The images of the simulations of the extreme combinations of air pressure and friction show a relationship between the air pressure and the penetration into the padding. For a lower air pressure value, the skater digs himself further into the padding as compared to a high air pressure value. Most likely, due to this deeper penetration into the padding he bounces back with a lower speed, so that his bounce back is also less far.

5. Discussion and conclusions

5.1 Discussion

In this research an existing numerical model was improved in order to be able to measure the influence of different padding variables on the injury risk of a skater. The model was updated to the latest version of the software in order to get it running and several changes were made. Firstly, another human model was chosen for the simulations. This human model has improved as compared to the model that was used previously in that it combines the detailed body part models that were previously only separate models and furthermore, active behaviour of the neck, spine, elbows and hips was added. Secondly, the padding model was improved by defining the padding materials more accurately, defining the contacts between the human model and the padding more transparent and re-defining the correlation between the air pressure and the mass flow rate.

Three injury criteria for the head, neck and spine were selected in order to measure the risk and severity of the injury incurred upon impacting the padding. These criteria cover the linear acceleration of the head, the shear forces and moments in the neck and the linear acceleration and deflection of the thorax and spine.

First, three real impact scenarios were modelled, in order to analyse whether the model simulates a crash in a realistic way. Varying results were seen in this phase. The bounce back of the skater was modelled to a very acceptable level. However, the rotational movement of the skater was modelled very accurately in one impact scenario and wasn't modelled at all in another. Possible explanations for that may be that there was a small, though crucial difference in the initial posture of the skater or that the skater had an initial rotational velocity that was not taken into account in the model. Overall it was seen that, whether the real crash was simulated very well or not so, the model did show responses that were all thought to be realistic in some impact scenario.

Then, tests were performed with varying air pressure and cover friction. The HIC and CTI did not show a correlation for any of the variables. The neck injury predictor gave an impression of the neck movement upon impact. Maximum values of the NFP and NEP show that upon impact the neck reaches maximum extension first at circa 60ms from the start of the impact, shortly followed by the maximum flexion. Furthermore, for the extension of the neck lowest values are found for the highest air pressure values and for the flexion of the neck the lowest values are found for the lowest air pressure values.

All injury criteria showed high peak values, indicating that many moderate to serious injuries would be incurred when impacting the padding in the modelled impact position. However, in reality only few serious injuries are occurring. It is believed that this may be due to the active behaviour of the skater. Even though an active human model is used, active behaviour only starts at the moment of impact and an increase of muscle stiffness happens after 140 to 200ms. A real skater sees his crash coming and can prepare active behaviour before the crash, such that at the moment of impact his muscles are already stiffer.

Forbes et al. (2007) also measured the HIC for varying air pressure and friction. In their results too there was no relation found between the HIC and the air pressure. They did find a relation between the HIC and the padding friction. For increasing friction increasing HIC values were observed. Simulations in their research gave maximum HIC values of 200 to 400 with some outliers. Major differences in the conditions in their research were a higher impact speed in their simulations (60km/h vs. 55km/h), a different impact angle (40° vs. 45°) and a different impact posture of the skater (lying on the back, impacting with the side first and lying on the side, impacting with the back first). It is most likely that the large differences in HIC results are due to the difference in posture of the skater. This was also observed in the different impact postures that were simulated in this research, where three different impact postures showed HIC values ranging from 206 to 822. The HIC values measured by Forbes et al. (2007) are closest to the HIC value that was measured in the present research for the first impact scenario of a skater impacting the padding in a sitting position, leaning far back, with his right side hitting the padding first.

5.2 Conclusions

A numerical model was chosen as a testing method and an existing air filled padding model was adjusted in such a way that it is ready to test the currently available Sidijk air filled padding with the latest MADYMO software. Additional validation test were done, which showed that the model is able to produce a realistic response for a given impact scenario. Therefore, the model is believed to be suitable for performing more padding tests.

The injury criteria that were used for evaluating the skaters injury risks did not show correlations for air pressure or friction for this impact scenario. This may lead to two conclusions: 1) there is no correlation between the air pressure or the cover friction and these injury criteria or 2) there is no correlation for these padding variables for this impact scenario. Simulations of more impact scenarios are needed to give answer to this matter. The simulations of three different impact scenarios did show that the Head Injury Criterion depends on the skater posture upon impact.

All three injury criteria showed high values, indicating great risks of incurring moderate to severe injuries. This may point to the high risk speed skaters have of incurring severe injuries. However, the amount of values pointing towards such high risks measured in this research was not in proportion to the amount of serious injuries that occurs in reality. An explanation for that is, that a real skater reacts much more active to a crash than this model does. Moreover, the active reaction of a skater comes already before the crash while the model reacts only when the impact has already happened. Therefore, the injury criteria calculated in the model can be used to compare different simulations, but cannot be used to interpret one on one the injury that a skater will occur in a real impact.

6. Recommendations

This research project has provided a numerical model that is suitable for the testing of padding parameters. Three validation tests have been done, followed by variation tests for one impact scenario and two padding variables. However, this project started with the intention of improving the current standards for ice rink protection systems, in order to reduce the number of (severe) injuries incurred by impacting the padding. More testing will have to be done in order to reach that goal. Follow-up research may go into several directions.

Firstly, the same variables could be used and the same injury criteria could be measured for other impact scenarios. Differences can be made in the initial posture of the skater, his impact speed or his impact angle.

Secondly, other padding properties can be varied. The literature study that was done in the first phase of this research project provides a list of padding properties for which the influence on the padding performance is yet unclear.

Furthermore, different factors can be measured. For that, the literature review also gives a list of possibilities. One can either choose to measure other injury criteria, or to go for completely different factors like the deformation of the padding or the energy absorption.

Then, the model can be further improved by modelling a real sheet that includes pre-stress from the attachment with Velcro straps. Moreover, new models could be made for a foam filled padding or for a short track padding. Finally, it would be interesting to model a mass start or marathon impact situation with more skaters falling at once. By doing that, it can be observed how the padding reacts to a larger mass representing multiple skaters impacting at once at the same place, or how it reacts to several masses representing several skaters impacting the padding at once at different places.

References

Bruinsma, Y. 2016. Ice Rink Protection Systems - Review of the Factors that Influence the Safety of Ice Rink Protection Systems and Corresponding Test Methods, MSc Literature Report.

Eppinger, R., Sun, E., Bandak, F., Haffner, M., Khaewpong, N., Maltese, M., Kuppa, S., Nguyen, T., Takhounts, E. and Tannous, R. (1999) 'Development of improved injury criteria for the assessment of advanced automotive restraint systems–II', *National Highway Traffic Safety Administration*.

FIM (2015) *2016 APD Certification Program.* Mies: Fédération Internationale de Motocyclisme (FIM).

Forbes, P. A., Ruimerman, R. and Stam, E. D. (2007) *Impact Protection in Sports - Improving Impact Protection for Long Track Speed Skating*, Helmond: TNO.

Forbes, P. A., Willems, J. W. M. and Vendrig, R. (2006) *Impact Protection in Sports - Development of Numerical Models to Describe Long Track Speed Skating Impacts*, Delft: TNO.

ISU (2012) *Communication No. 1726 - Short Track Speed Skating Rink Board Padding and Safety for Skaters.* Milan: International Skating Union (ISU).

ISU (2016) *ISU Skating Channel*. Available at: http://www.eurovisionsports.tv/isu/ (Accessed: 8 March 2017).

KNSB (2017) *Unpublished video material* (Accessed: 8 March 2017).

MADYMO (2015a) *Human Body Models Manual, Release 7.6*: TNO.

MADYMO (2015b) *Reference Manual, Release 7.6*: Tass International.

MADYMO (2015c) *Theory Manual, Release 7.6*: Tass International.

Maw, S. and Johnston, C. (2005) *Summer 2005 Short Track Speed Skating Crash Pas Engineering Pilot Study Results*: Olympic Oval; Faculty of Kinesiology; University of Calgary.

Maw, S. and Johnston, C. R. 'The Design of Foam Crash Pads for Short Track Speed Skating on Boarded Rinks', *2nd International Conference of the SportSURF Network*, Loughborough University, April 2010.

Mehler 2008. Technical datasheet No.: 1040.2. Mehler Texnology.

Mehler 2013. Technical datasheet No.: 1255.4. Mehler Texnologies.

NOS (2017) *NOS Studio Sport*. Available at: http://www.npo.nl/ (Accessed: 8 March 2017).

Schmitt, K., Muser, M. H. and Niederer, P. 'A new neck injury criterion candidate for rear-end collisions taking into account shear forces and bending moments'. *Proceeding of the 17th International Technical Conference on the Enhanced Safety of Vehicles*.

Shojaati, M. 'Correlation between injury risk and impact severity index ASI'. *Proceedings of the 3rd Swiss Transport Research Conference Monte Verita/Ascona*.

Tass-International (2017): Tass International. Available at: https://www.tassinternational.com (Accessed: Januari 16 2017).

Appendix A. Selection of testing method

In the literature study several testing methods have been found that can be used for testing of protective paddings. The International Skating Union (ISU) recommends the use of a drop test to evaluate the performance of paddings used for short track speed skating (ISU, 2012). Previous research on this topic has been done using pendulum tests (Forbes et al., 2007, Maw and Johnston, 2005, 2010) and, furthermore, a numerical model has been developed for this purpose (Forbes et al., 2006, 2007). In motorsports the International Motorcycling Federation (Fédération Internationale de Motocyclisme, FIM) requires testing of paddings, similar to those used in speed skating, with a crash test dummy (FIM, 2015).

Two aspects are important to determine whether a method is suitable or not for this research. First, the padding should be well represented, in order to get good results on the padding performance upon impact. Secondly, the impacting object should be able to properly represent a skater. The sliding movement of the skater towards the padding, the posture of the skater and the injury response of the body are points of attention.

A.1 Drop test and pendulum test

A drop test is done using a mass which is released from a certain drop height to fall freely onto the padding. In a pendulum test a mass is connected to the end of a rigid bar of which the other end is connected to a hinge on the ceiling. The mass is lifted up and released to swing towards the padding in a prescribed circular motion. For both of these testing methods it holds that testing can be done on a real padding, so that no assumptions have to be made on the padding materials, dimensions, attachment methods, etc. However, in a drop test the padding is lying flat on the ground and will not respond to the impact as it would when standing upright and supported like it is on the ice rink.

Furthermore, the skater is not properly represented in both of these methods. In a drop test the movement of the mass towards the padding can only be monitored and not well controlled and in a pendulum test the mass can only move in a prescribed circular path. Therefore, the movement of the skater before and after the impact cannot be simulated in a realistic way. Moreover, both of these methods make use of one rigid body which cannot be put into several skater postures and cannot represent the injury response of the body. Both methods are therefore considered to be unsuitable for this research.

A.2 Crash test versus numerical model

The use of a numerical model and a crash test dummy are both more accurate representations of the real situation.

A crash test dummy is an instrumented humanoid that can be launched towards an actual padding. Existing dummies are designed to measure in one normal direction. In this research the goal is to move the skater towards the padding under a certain impact angle other than 90 degrees, causing that two normal directions are involved in the movement. Therefore, existing dummies cannot properly measure the injury response of the body under the testing conditions of this research. It is, however, possible to design a new dummy-like measurement instrument that can measure under an angle other than the normal directions.

In a numerical model, the skater and the padding both have to be modelled as accurate as possible. Thereafter, a simulation can be done in which the skater model is impacting the padding model. A model that can be used for simulations of this kind has already been developed by Forbes et al. (2006) and is available to be used in this research.

When it comes to the representation of the padding, using a crash test dummy is favoured over a numerical model because with a crash test dummy a real padding can be impacted, while in a numerical model assumptions have to be made in order to model a padding.

Looking at the representation of the skater, making a decision is more difficult. A crash test dummy can be launched under controlled circumstances in a chosen direction and can freely move after the impact in the natural bounce back direction. Therefore, the movement of the skater can be well represented. Crash test dummies are instrumented humanoids, consisting of a head, neck and trunk, that are designed to measure parameters that are necessary for the evaluation of the injury response of those body parts. The skater posture can be represented to the extent that the front, side or rear of the body impacts the padding first. The effect of the limb position cannot be taken into account, because those body parts are absent in a dummy.

The software that is used to build a numerical model includes full human models. These human models consist of a full body skeleton modelled by rigid bodies that are connected by joints and furthermore muscle activity is included. The models are based on biomechanical data that was obtained from literature and they have been validated using data from volunteer and post mortem human subject (PMHS) impact tests (MADYMO, 2015a). The human models exceed the crash test dummies in that they can simulate all skater postures due to the full body representation and that they are able to simulate and measure intermediate impact directions, i.e. sliding directions of an angle <90 degrees involving two normal directions. Therefore, the parameters that are necessary for calculating the injury response can be properly measured under all impact directions. Moreover, calculation of several injury criteria can be done within the software itself.

A.3 Final selection

It was already concluded that, based on their insufficient representation of the skater aspects, the drop test and pendulum test are unsuitable for this research. The numerical model and the crash test are more evenly matched. Table 6 summarizes the pros and cons of those two methods.

Table 6 – Pros and cons of the crash test and numerical model

	Availability	Padding representation	Skater representation		
			Movement	Posture	Injury response
Crash test	-	+	+	+/-	-
Numerical model	+	+/-	+	+	+

The crash test and numerical model both have the ability to represent the real situation well. A crash test is preferred based on the fact that for such a test a real padding can be used. A numerical model is favoured for its good representation of the skater. A decision is made in favour of the method that performs the best over-all. It is believed that in a crash test the skater representation is weak, even though the padding representation is very strong. In a numerical model the skater representation is of a high level and also the padding representation can be modelled to an acceptable level. Therefore, the numerical model is the best performing method for the purpose of this research.

Appendix B. Images of real crashes and simulations

B.1 Impact scenario 1

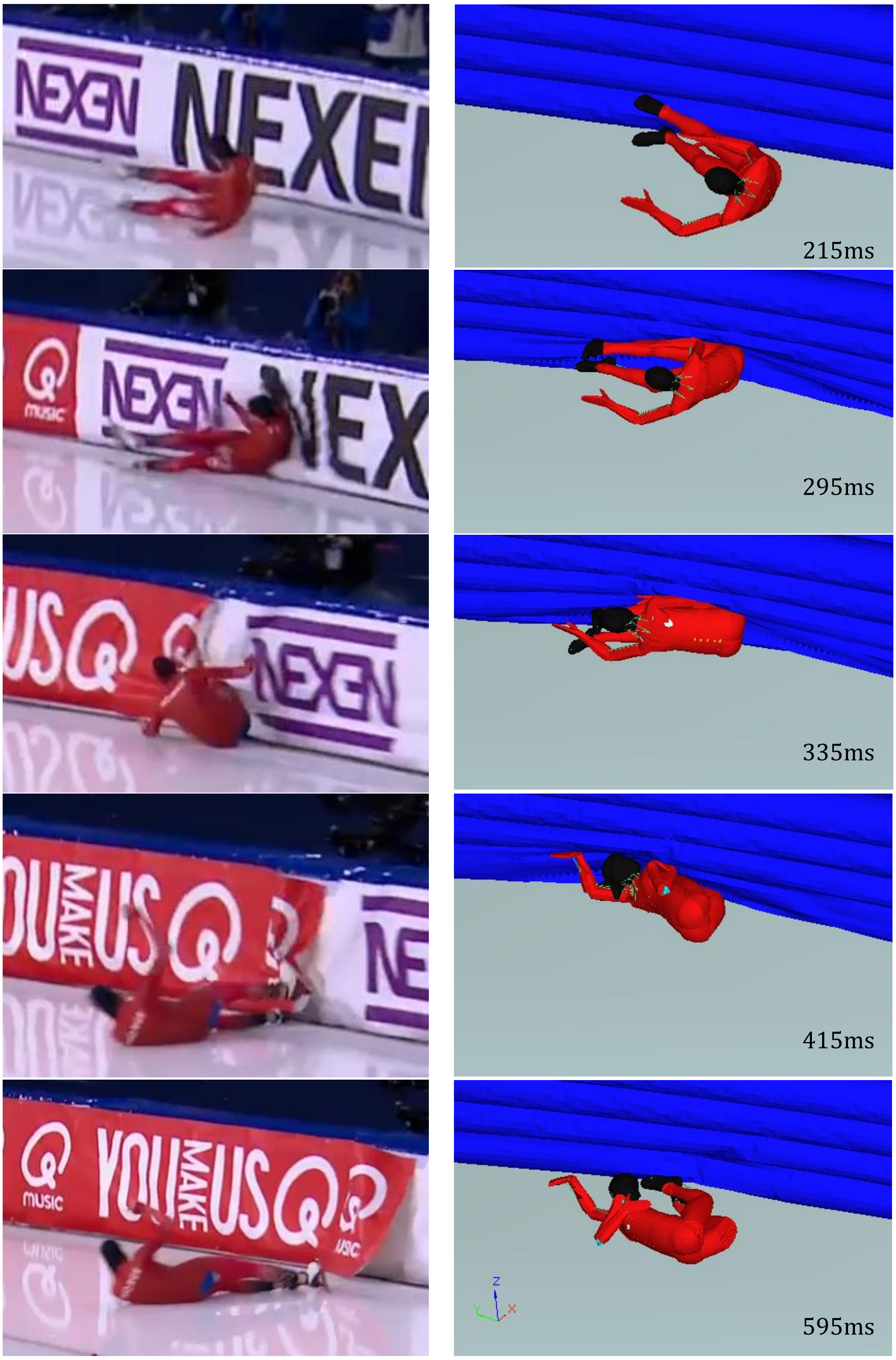

Figure 17 – Images of impact scenario 1
(left: real impact (ISU, 2016); right: simulated impact)

B.2 Impact scenario 2

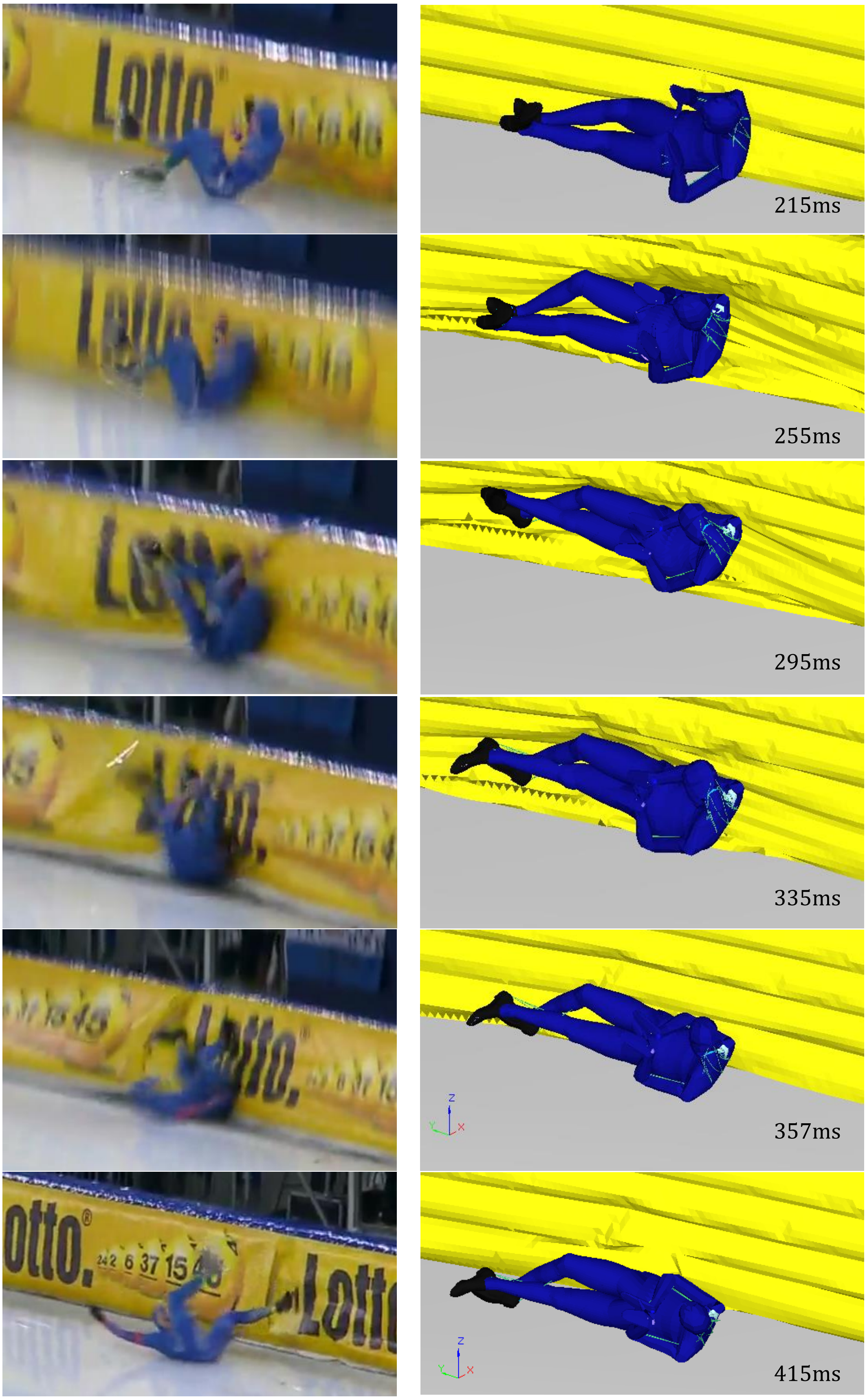

Figure 18 – Images of impact scenario 2
(left: real impact (NOS, 2017); right: simulated impact)

B.3 Impact scenario 3

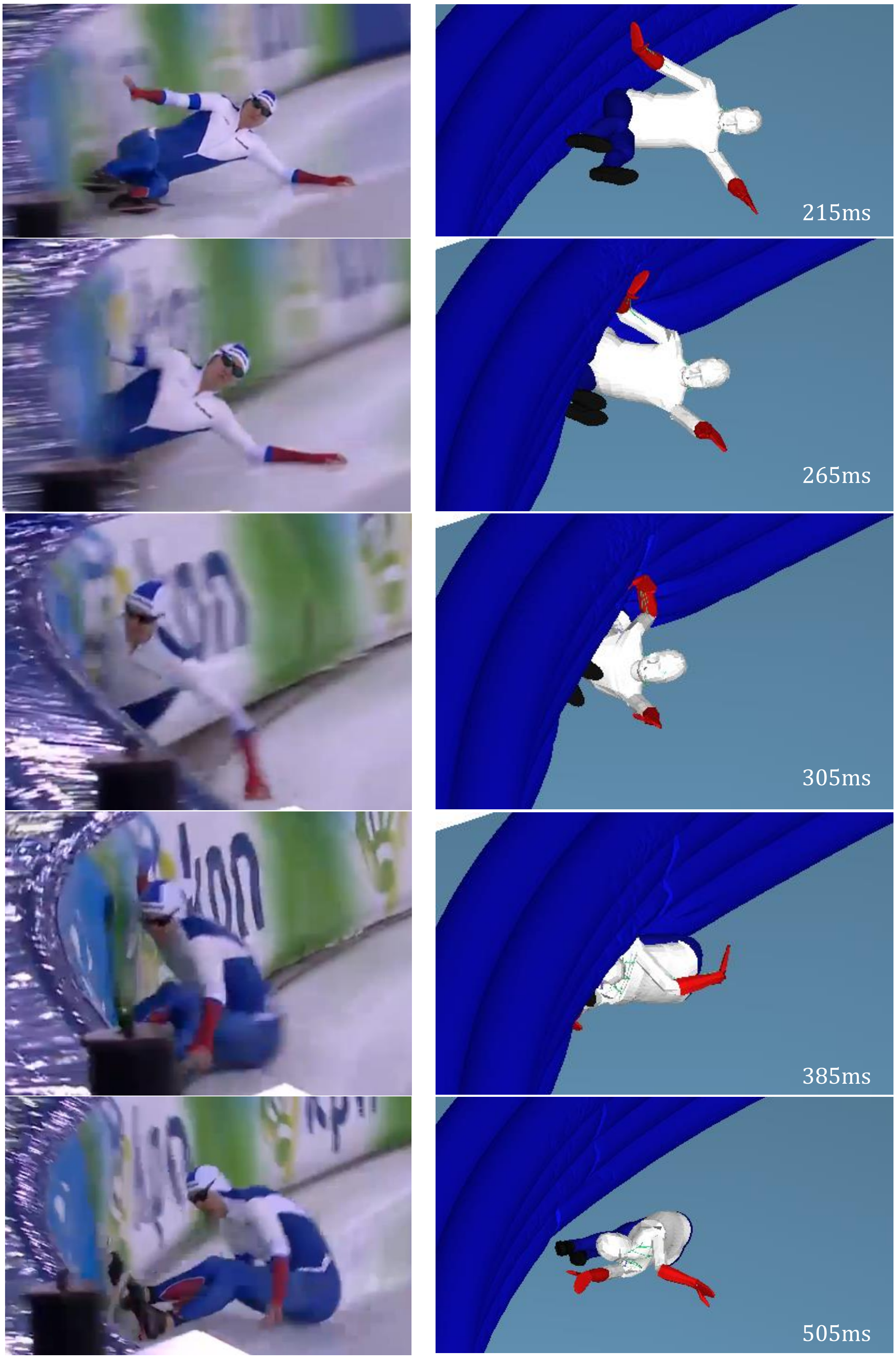

Figure 19 – Images of impact scenario 3
(left: real impact (ISU, 2016); right: simulated impact)

Appendix C. Data from injury criteria

C.1 Head Injury Criterion (HIC)

Table 7 – HIC-15 values for all combinations of air pressure and friction[1]

		Friction			
		0.3	**0.5**	**0.7**	**0.9**
Pressure [Pa]	**600**	538.25	754.92	955.72	874.76
	1200	767.95	870.45	705.71	525.60
	1800	679.69	795.69	848.79	726.37
	2400	689.67	947.89	719.48	891.72
	3000	558.31	776.93	640.28	766.21

[1]Values that exceed the threshold of 700 are marked in red

C.2 Neck injury predictor Nkm

Table 8 – Maximum Nkm values for all combinations of air pressure and friction[1,2]

		Friction			
NFA		**0.3**	**0.5**	**0.7**	**0.9**
Pressure [Pa]	**600**	0.11045	0.60808	0.67064	1.11430
	1200	0.11045	0.21668	0.11149	0.11584
	1800	0.43324	0.80326	0.95334	0.76581
	2400	0.31691	0.53726	0.11045	0.57817
	3000	0.11045	0.28113	0.11045	0.11045
NEA					
Pressure [Pa]	**600**	0.10260	0.17498	0.04682	0.42804
	1200	0.19514	0.10929	0.29863	0.32532
	1800	0.18206	0.12809	0.05003	0.49971
	2400	0.32905	0.12956	0.22602	0.32322
	3000	0.33314	0.04682	0.27563	0.51349
NFP					
Pressure [Pa]	**600**	0.87441	0.75235	0.83184	0.97463
	1200	0.96626	0.74589	0.70361	0.90120
	1800	0.96785	0.71532	1.27560	0.76134
	2400	1.10570	0.86327	1.01330	0.85169
	3000	1.19690	1.03840	1.09570	0.62731
NEP					
Pressure [Pa]	**600**	0.77988	0.94226	1.17810	0.90190
	1200	0.89723	0.97379	1.11670	1.03910
	1800	1.04200	1.00710	1.44860	0.88655
	2400	0.77648	1.00940	1.03620	1.04500
	3000	0.80386	0.93858	0.90618	0.90879

[1]Values that exceed the threshold of 1 are marked in red
[2]Values that occur outside the time window of 200ms after the start of impact are marked in grey

C.3 Combined Thoracic Index (CTI)

Table 9 – CTI values for the first rib layer for all combinations of air pressure and friction[1]

Ribs 1		Friction 0.3	0.5	0.7	0.9
Pressure [Pa]	600	0.98033	0.90295	0.81553	0.81384
	1200	0.82050	0.81384	0.92375	0.81482
	1800	1.30800	0.81384	0.81384	0.81385
	2400	1.27570	0.81384	0.81384	0.81384
	3000	0.88325	1.07860	0.84065	0.82835

[1]Values that exceed the threshold of 1 are marked in red

Table 10 – CTI values for the second rib layer for all combinations of air pressure and friction[1]

Ribs 2		Friction 0.3	0.5	0.7	0.9
Pressure [Pa]	600	0.69003	0.69484	0.69003	0.69003
	1200	0.69865	0.86127	0.69003	0.73832
	1800	1.04580	0.69003	0.72624	0.69200
	2400	0.69003	0.70202	0.69003	0.69003
	3000	0.69003	0.69003	0.71788	0.77922
Ribs 2 right					
Pressure [Pa]	600	0.82537	0.70527	0.68026	0.68026
	1200	0.76946	0.70093	0.68026	0.69125
	1800	0.85236	0.74220	0.77045	0.68577
	2400	0.75633	0.72654	0.68026	0.68026
	3000	0.74705	0.72303	0.73702	0.74341
Ribs 2 left					
Pressure [Pa]	600	0.69830	0.78974	0.61689	0.79153
	1200	1.17600	1.26260	0.74830	0.78150
	1800	1.34310	1.01120	0.71107	0.76782
	2400	0.74063	0.85246	0.71667	0.69070
	3000	1.32190	0.79504	0.71222	0.80977

[1]Values that exceed the threshold of 1 are marked in red

Table 11 – CTI values for the third rib layer for all combinations of air pressure and friction[1]

Ribs 3		Friction 0.3	0.5	0.7	0.9
Pressure [Pa]	600	0.72788	0.73860	0.60584	0.68851
	1200	0.91709	1.10100	0.76220	0.70731
	1800	0.92749	0.77279	0.67526	0.70873
	2400	0.83507	0.85073	0.85684	0.75196
	3000	0.88440	0.80668	0.85699	0.68154
Ribs 3 right					
Pressure [Pa]	600	0.71816	0.70926	0.64584	0.63878
	1200	0.81696	0.71475	0.72905	0.64510
	1800	0.88829	0.73748	0.84935	0.64415
	2400	0.69793	0.65376	0.76276	0.70978
	3000	0.70368	0.74872	0.75688	0.59922
Ribs 3 left					
Pressure [Pa]	600	0.77662	0.90019	0.76201	1.02590
	1200	0.76327	0.91775	0.87405	0.81326
	1800	1.03640	0.82893	0.66941	0.75189
	2400	0.78536	0.96457	1.04470	1.01770
	3000	1.00780	0.96119	1.05880	0.78182

[1]Values that exceed the threshold of 1 are marked in red

Table 12 – CTI values for the fourth rib layer for all combinations of air pressure and friction[1]

Ribs 4		Friction 0.3	0.5	0.7	0.9
Pressure [Pa]	600	1.04000	1.04000	1.04000	1.04000
	1200	1.04000	1.05720	1.15580	1.05550
	1800	1.05650	1.04000	1.04000	1.04000
	2400	1.05740	1.04000	1.04000	1.10590
	3000	1.05540	1.04000	1.04000	1.04000
Ribs 4 right					
Pressure [Pa]	600	1.02400	0.91473	0.81057	0.85871
	1200	0.91392	0.77375	0.98572	0.83592
	1800	1.17580	0.84566	1.06710	0.86751
	2400	0.97640	0.75848	0.92313	0.91394
	3000	0.96096	0.91263	1.04500	0.92758
Ribs 4 left					
Pressure [Pa]	600	0.86751	0.62240	0.70818	0.81421
	1200	0.93982	1.10420	0.74665	0.74408
	1800	1.64150	0.82742	0.75238	0.61319
	2400	0.90878	0.80390	0.86039	0.82322
	3000	0.88344	0.70430	0.69759	0.63835

[1]Values that exceed the threshold of 1 are marked in red

Appendix D. Images of simulated impact scenarios

D.1 Fixed connection – Friction = 0.3

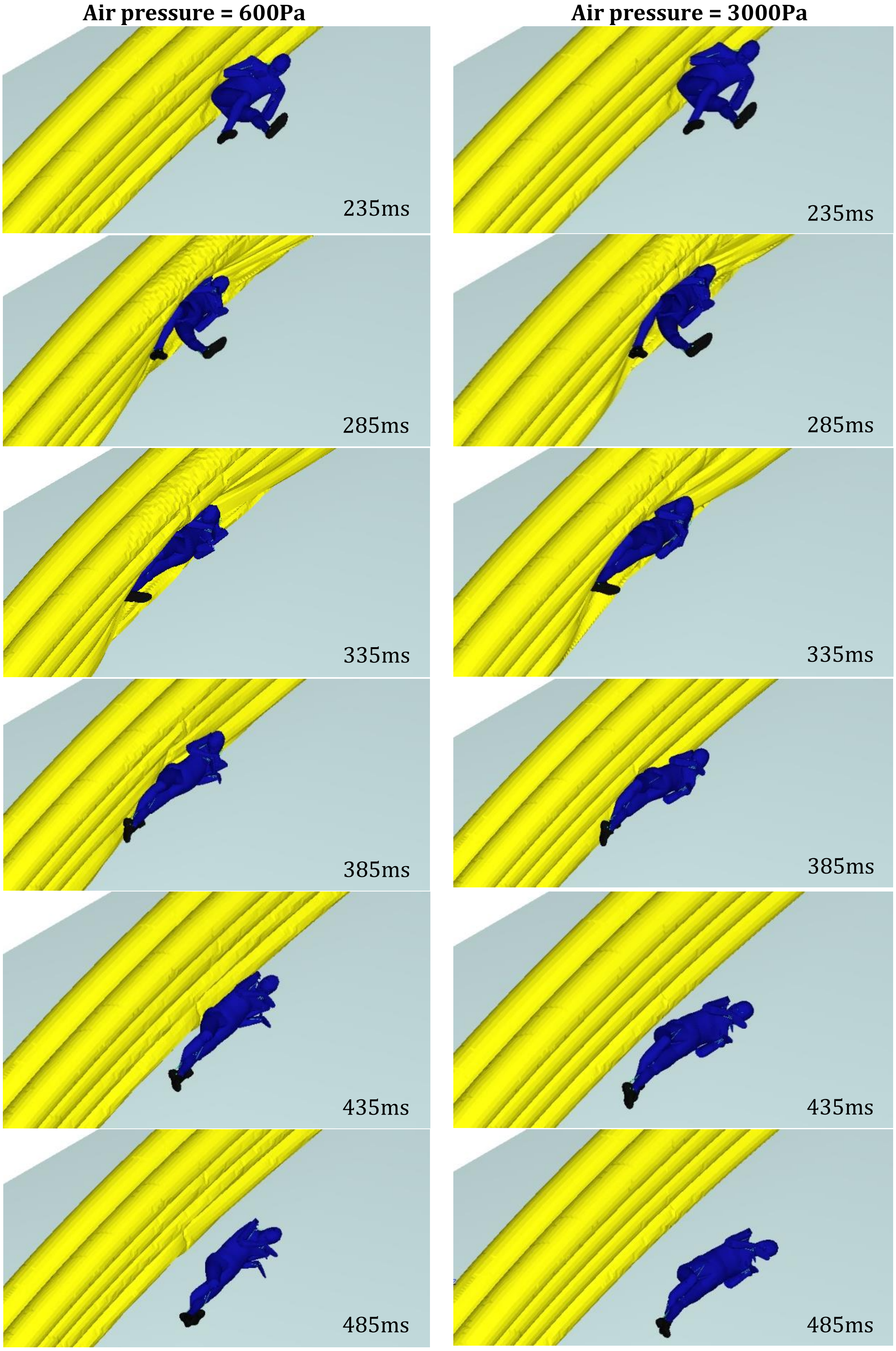

Figure 20 – Images for simulations with a fixed ground connection, a friction of 0.3 and an air pressure of 600Pa (left) and 3000Pa (right)

D.2 Fixed connection – Friction = 0.9

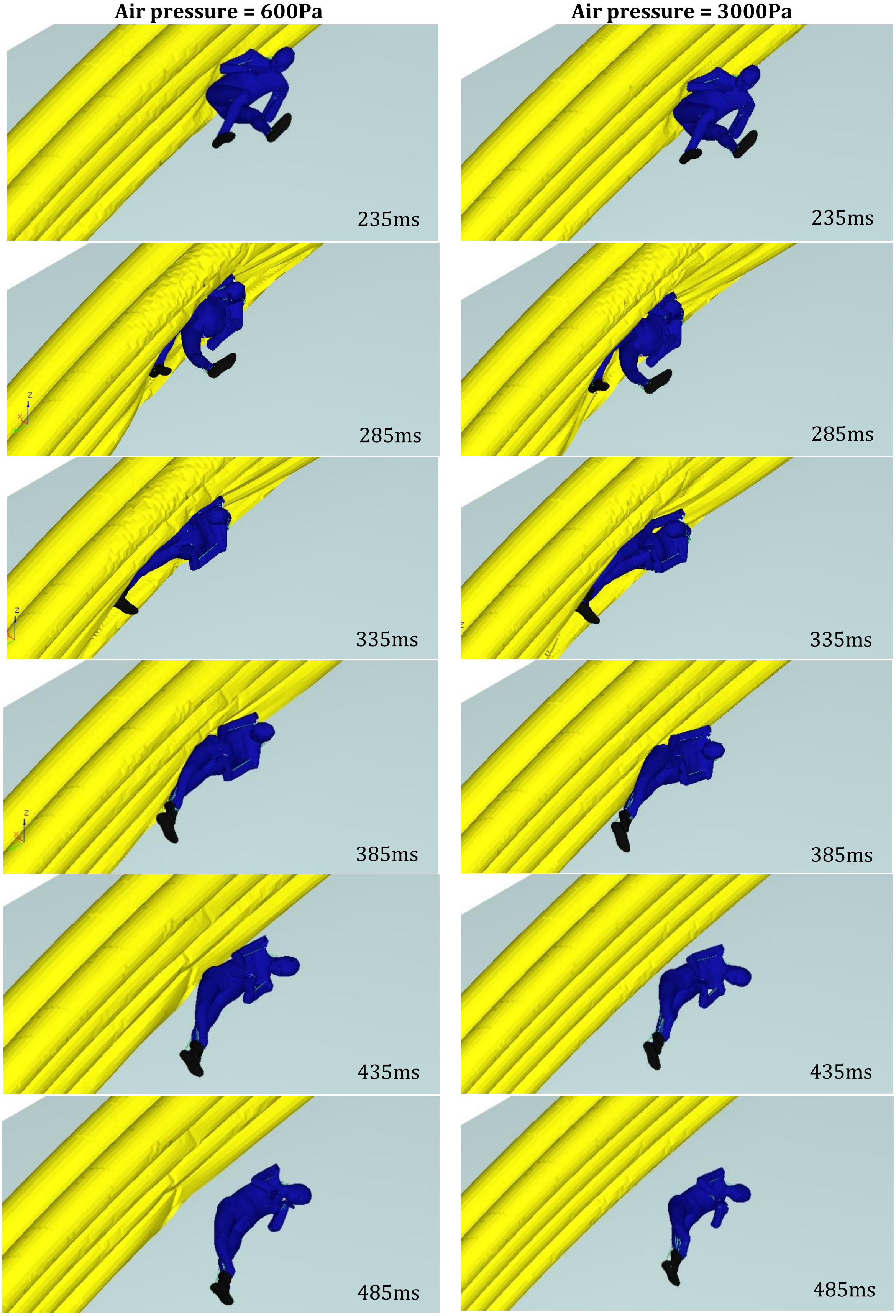

Figure 21 – Images for simulations with a fixed ground connection, a friction of 0.9 and an air pressure of 600Pa (left) and 3000Pa (right)